Effects of Red Blood Cell Aggregation on Microparticle Margination in Human Blood

Mark Stroobach

Supervised By:
Prof. Marianne Fenech

Thesis submitted in partial fulfillment of the requirements for the

Master of Applied Science in Biomedical Engineering Degree

uOttawa

University of Ottawa

Ottawa, Ontario, Canada

Abstract

Margination is the migration of particles in a channel towards the outer walls of the channel. In blood microcirculation, studying the margination of microparticles is important to understand platelet migration and the kinetics of drug delivery. Many new topics in drug delivery research examine the slow release of drugs through micro particles, such as micelles. The margination of such drug carriers is related to tissue absorption and, consequently, to the efficiency of drug delivery. We hypothesized that the intensity of red blood cell (RBC) aggregation will change the level of margination in a cylindrical channel. RBC aggregation is the reversible process of RBCs clumping together over time, under low fluid shear rate. A higher level of aggregation means that this clumping occurs more quickly.

The goal of this thesis is to design an experiment that measures the level margination of microparticles and the effect that RBC aggregation has on margination, in a controlled *in vitro* environment. Fluorescent microparticles were added to human blood preparations. The aggregation properties of the blood preparation were modulated by the addition of a macromolecule (Dextran 500). The blood preparations were injected into PDMS microfluidic devices that were modified to have circular channels in order to better mimic the geometry of physiological microcirculation.

We designed a circular microchannel that worked to capture the marginating microparticles and it was found that the level of margination of the microparticles increased with an increase in aggregation of the RBCs. This increase in margination was especially sensitive to aggregation levels in the range of physiological aggregation levels of whole blood, suggesting that aggregation plays an important role in margination *in vivo*.

Acknowledgements

I would like to thank all the people who helped me with the writing of this research project.

Firstly I would like to thank the members of my family and my fiancé for their help and support.

Secondly, I would like to thank Laura for all the work she put in, proofreading and fixing my silly mistakes.

And lastly, I would like to thank Marianne, my thesis supervisor, for always being there to help guide me in my work and my writing.

Without any of them, this work may never have been finished in time.

I. Table of contents

II. List of figures

III. List of tables

IV. Nomenclature

Q	flow rate (m^3/s)
h	channel height (m)
w	channel width (m)
μ	dynamic fluid viscosity (Ns/m^2)
L	length (m)
p	pressure (N/m^2)
τ	shear stress (N/m^2)

V. Acronyms

RBC	Red blood cell: also called erythrocytes
WBC	White blood cells: also called leukocytes
PBS	Phosphate buffered saline
CFL	Cell free layer
HF	Hydrofluoric acid
UV	Ultraviolet: a range of electromagnetic radiation
PDMS	Polydimethylsiloxane: Silicon based organic polymer
AI	Aggregation index
AUC	Area under the curve
AAC	Area above the curve

VI. Definitions

Dextran: a complex branched polysaccharide of glucose. It is of varying molecular weight; when referring to dextran in this study, it is to dextran with a molecular weight of 500 kDa (Dextran 500), unless otherwise specified.

Hematocrit: the ratio of RBCs to the total volume of the blood.

Margination: The act of particles in blood stream moving towards the walls of the channel.

RBC aggregation: reversible clumping of RBCs under low shear forces or at stasis.

RBC deformation: the ability of red blood cells to deform in response to stress.

1 Introduction

Blood is an essential fluid in the human body; it transports nutrients and respiratory gases to all cells in the body. It is very complex and contains many types of particles in suspension. A complete understanding of the physical properties of blood is important to understand health, as well as the properties of some diseases that affect the blood. One important property of blood and blood flow is margination, which is the propensity of particles in blood to move towards the walls of the blood vessel. Studies have shown the importance of the margination of platelets and white blood cells in wound healing, in hemostasis and at sites of inflammation and infection (Carboni et al. 2014).

It is believed that the aggregation of red blood cells, (the reversible clumping of RBCs under low shear stresses) may have an important role on particle margination; however, this relationship is not yet fully understood. It has been shown that human blood aggregation increases during tissue inflammation, as well as in other pathological or diseased states, as has been observed in diabetic patients and in cases of sepsis (Nash et al. 2008). Understanding how aggregation affects margination may be important in order to develop potential treatments (Baskurt et al. 2012).

Furthermore, the margination of drug particles is important to drug delivery. Drug-tissue interaction occurs at the vessel walls, therefore, a higher level of margination at one location in the body would result in more drugs being absorbed there, compared to a location where margination was lower.

1.1 Research question

What is the role of RBC aggregation in particle migration and can a method be established to study this relationship, under conditions that are as close to physiological as possible?

1.2 Hypothesis

Based on the study by Nash et. al (2008), which showed that the level of RBC aggregation was positively correlated with the level of leukocyte and platelet margination, we hypothesize that RBC aggregation enhances the margination of particles under low shear in the microcirculation, in circular microchannels.

1.3 Objectives

The primary objective of this study is to assess the effect of aggregation on particle migration. We will measure this effect within circular microchannels and at flow velocities relevant to physiological flow in the microcirculation. To be able to do so, the specific objectives of this master thesis are then:

1) to determine an appropriate methodology to fabricate round microchannels in PDMS,

2) to develop a methodology using streptavidin and biotin to capture particles that have moved toward the wall, and finally

3) to perform a comparison of particle migration in round microchannels for four different levels of RBC aggregation and at four different flow velocities.

2 Background

In this chapter, we will discuss background information necessary to understanding blood flow and the fabrication of round channels in preparation for the experiments.

2.1 Blood physiology and flow properties

2.1.1 Particles in the fluid

Blood is composed of cells (red blood cells, white blood cells, and platelets) that are suspended in a liquid called plasma. These elements are described in detail in the following.

Blood plasma is the carrier medium that blood cells travel in. It is composed mostly of water (~90%) as well as multiple types of dissolved proteins and nutrients. Plasma carries proteins such as fibrinogen, which helps in the formation of blood clots, and insulin, which helps control blood sugar levels. It also carries sugars and nutrients such as fats to and from their storage location. Plasma contains a large amount of ions dissolved into it, such as potassium, calcium, sodium and chloride, which are supplied to the tissues that need them, and maintain an electrolytic balance with electro-active tissues, such as nerve and muscle cells. Plasma also controls blood pH levels and CO2 levels with excess CO2 expelled through the gas exchange membrane of the lungs and exhaled (Hall & Guyton 2011).

Erythrocytes

Erythrocytes, also known as red blood cells (RBCs) are the oxygen carriers of the body. They are very rich in the protein hemoglobin. Hemoglobin is the main carrier of oxygen in RBCs. The iron ion in hemoglobin will bind to oxygen in an oxygen rich environment (i.e. the gas exchange tissue of the lungs) and release it in an oxygen poor environment (i.e. other bodily tissues) supplying oxygen to the body. Under normal atmospheric conditions, hemoglobin is saturated at a rate greater than 95% (i.e. more than 95% of all hemoglobin units will be carrying

an oxygen molecule) in the lungs. This saturation rate decreases rapidly with decreased atmospheric pressure (Hall & Guyton 2011).

Red blood cells are derived from myeloid progenitor cells, which are derived from multipotent hematopoietic stem cells in the bone marrow. In order to make room for all of the hemoglobin proteins, which account for more than 90% of an RBC's proteins, the RBC loses its nucleus in its juvenile stage. This also allows the RBC to stay small and flexible so that it may easily traverse the microcirculation; however, it prevents the cell from making any new proteins or to divide (mitosis). It is for this reason that they must be formed in the bone marrow and then be delivered to the vasculature. Once an RBC enters the vasculature, all it can do is transport oxygen and other molecules until it dies. Since it cannot regulate itself when it dies (unlike most cells, which will undergo apoptosis), it must be removed from the vasculature by the spleen, liver or lymph nodes. These organs will filter out old or dead RBCs from normal, healthy ones and recycle them through phagocytosis by macrophages in order to prevent waste from dead cells building up and damaging the blood vessels. Most RBCs will be recycled before they undergo hemolysis, the rupturing of RBCs (Hall & Guyton 2011).

Normal, healthy red blood cells are biconcave discoids. They are generally 6-7 μm in diameter and 2-3 μm thick. Their shape gives them a great amount of flexibility. This ability to deform in response to stress is referred to as RBC deformation. Their deformation allows them to bend nearly in half in order to pass through capillaries that are smaller than their normal diameter.

The percentage of volume that RBCs occupy in whole blood is called hematocrit. Under physiological conditions, in large arteries or veins, the hematocrit is generally around 45%, meaning that of the total volume of blood, 45% of it is comprised of RBCs. In smaller diameter

vessels the hematocrit is lower, due to a phenomenon known as the Fåhræus effect and the cell free layer that forms in the parent vessel of the smaller branches.

Thrombocytes

Thrombocytes, also known as platelets, are also derived from myeloid progenitor cells in the bone marrow, but from those that differentiate into megakaryocytes. Megakaryocytes are the precursors for platelets; they are very large cells from which small sections of the membrane pinch together and break off. These broken off pieces become platelets (Hall & Guyton 2011).

Platelets are primarily involved in blood coagulation in order to stop bleeding when a vessel is injured. Platelets are generally one to two micrometers in diameter, and as they were broken off from a larger cell, they have no nucleus. When formed, platelets vary slightly in size, but are on average spherical and around 1 µm in diameter (Hall & Guyton 2011).

Platelets also undergo margination, especially in areas where the blood vessels are damaged. This allows the platelets to congregate more efficiently around the damage and form a clot, promoting healing and reducing bleeding.

Leucocytes

Leucocytes, also known as white blood cells, are all cells found in the blood derived from the multipotent hematopoietic stem cells that are not erythrocytes or thrombocytes. There are two main categories of leucocytes based on their cell lineage. The first is lymphoid cells from the lymphoid progenitor cell line, which includes B cells, T cells and natural killer cells. The second is myeloid cells from the myeloid progenitor cell line, which include basophils, neutrophils, eosinophils and monocytes. Monocytes can differentiate again into macrophages or other immune cells (Hall & Guyton 2011).

White blood cells are significantly larger than red blood cells. They are circular and have diameters between 10 and 30 micrometres, depending on their type. Their main responsibility is

immune function; lymphocytes in particular are the most important players in adaptive immunity, and detect antigens and produce antibodies for the antigens of foreign substances such as bacteria (Hall & Guyton 2011).

White blood cells also experience margination in blood vessels, especially near sites of inflammation or infection; their margination allows them to reach the walls of the channel and adhere (Freund 2007). Once adhered, they will roll along the vessel until they reach the site of inflammation or infection where they will work to repair the site (Freund 2007).

2.1.2 Non-Newtonian fluids

Newtonian fluid vs. non Newtonian

Whole blood is a non-Newtonian fluid. For a Newtonian fluid, the shear stress is linearly proportional to the applied shear rate, and its viscosity is constant, even with varying shear rate. A non-Newtonian is different in that its viscosity is dependent on the shear rate. Blood is a shear thinning fluid, meaning that as the shear rate increases, the fluid viscosity decreases. The non-Newtonian behaviour of whole blood is a result of the behaviour of the particles suspended within it – blood plasma, which contains no particles, is a Newtonian fluid. In whole blood, particle phenomena including RBC aggregation and deformation contribute to the fluid's non-Newtonian properties and affect the blood flow physics.

Shear

Shear stress is the tangential force of the flowing blood on the endothelial surface of the blood vessel and on the cells in the blood. An ideal Newtonian fluid, that is, one that is incompressible and frictionless, exhibits a non-turbulent, laminar pattern of flow at lower flow velocities. In a cylindrical tube, the resulting wall shear stress τ of laminar flow of a using the Poiseuille formula is:

$$\tau = \frac{4\mu Q}{\pi r^3}, \quad 1.$$

where μ is viscosity, Q is flow rate and r is radius of the tube.

Viscosity

Viscosity is a measure of the ability of the fluid to flow. Higher viscosity means that the fluid will exhibit a greater resistance to a force applied in parallel with the flow, which results in the fluid being thicker and flowing more slowly than a fluid with lower viscosity, if both are driven by the same pressure gradient. For shear thinning fluids, such as blood, increasing the applied shear rate causes the fluid viscosity to decrease. Whole blood also exhibits thixotropic behaviour, meaning that the blood's stress history influences its current viscosity. Consequently, the viscosity of blood undergoes a time-dependent change as blood experiences shear stress.

2.1.3 Aggregation

Most mammalian red blood cells, including human red blood cells have a tendency to form aggregates or cell clusters when under low shear forces or at rest. Initially, these are "face-to-face" linear adhesions of RBCs that resemble stacks of coins. Individually, these coin stack structures are known as rouleaux. The number of RBCs in a rouleaux can vary widely with branching often occurring (Baskurt et al. 2012). The flat surface of the discoid RBCs give them a large surface area to make contact and stick to each other. Rouleaux formation takes place only in suspensions of RBCs containing high-molecular, fibrillar proteins or polymers in the suspending medium. The most important protein causing rouleaux formation in plasma is fibrinogen (Blombäck 1996). RBCs suspended in simple salt solutions do not form rouleaux (Baskurt et al. 2012).

Two phenomena have been proposed to explain the face-to-face adhesion observed of RBCs. The first, more widely accepted possibility is termed "the depletion method": due to the lower concentration of other molecules near the cellular membrane compared to the surrounding plasma, an osmotic pressure difference generates an attractive force between two adjacent RBCs, weakly holding them together when they are face to face (Baskurt et al. 2012). The second possibility is that the adhesion is due to molecular bonding between RBCs at the cellular membrane. In both cases, the closer the RBCs are to each other and the more surface area they have in contact with each other, the stronger the adhesion will be and higher shear stresses will be required to separate them.

Effects of Aggregation on Health

Aggregation increases under conditions of inflammation, which is a complex response to harmful stimuli and involves the innate immune system. This is partly due to the increase of fibrinogen. It is thought that higher levels of aggregation may cause an increase to blood flow to the damaged sites and improve healing from the increase of white blood cells and platelets flowing there (Baskurt et al. 2012).

Causes of low and high aggregation

Aggregation forms from a balance of the forces promoting aggregation and the forces promoting disaggregation, the reverse process of aggregation by which an aggregate separates into individual RBCs, or smaller aggregates. Disaggregation can be caused by many factors including shear forces, surface charge density and membrane strain on the RBCs (Baskurt et al. 2012).

As mentioned, proteins in the blood plasma are required for RBC aggregation; RBCs will not form any aggregates or rouleaux in a salt solution. Fibrinogen, a glycoprotein, with a molecular mass of approximately 340 kilo Daltons (kDa), is the most potent aggregation inducer

found in the blood plasma. It is synthesized in the liver and in normal plasma, and is normally found in concentrations of 2-4 mg/mL in the blood. It is also an important factor in blood clotting and coagulation by being converted from soluble fibrinogen into insoluble fibrin strands which are cross-linked together to form a clot. Fibrinogen is also an acute phase protein, meaning that its concentration will increase due to any sort of inflammation in the body as part of the acute phase reaction. It can also increase in concentration due to several other diseases (Baskurt et al. 2012). Other blood plasma proteins that may have an effect on aggregation include immunoglobin G (IgG), immunoglobin M (IgM), C - reactive protein and albumin.

Shear forces

Sufficiently high levels of shear force on RBC aggregates will cause them to disaggregate: the shear force will act against the attraction force that occurs in aggregation, overwhelming it and separating the red blood cells.

Viscosity

Higher aggregation will also increase the viscosity of the blood due to the larger aggregates of RBCs that form.

2.1.3.1 *Measuring aggregation*

Aggregation can be measured using a device called an aggregometer. An aggregometer normally only needs a small sample of blood, around 5-10 µL to accurately measure aggregation. There are several different means by which an aggregometer can measure aggregation; however, the method used here is an optical method. In this method, the blood sample is injected by pipette into a well on a single-use chip, which also has a magnetic stirring bar already placed inside. The chip containing the blood sample is inserted into the aggregometer. The aggregometer shines a light (wavelength = 910 nm) of a specific intensity through the blood

sample, then the pre-placed magnetic stirring bar rotates rapidly, disaggregating all of the red blood cells inside the chip. When the bar stops, the RBCs will slowly aggregate and clump together. This aggregation will lower the total surface area the RBCs cover in the chamber, allowing more light to pass through the chip, through the gaps between aggregates. The machine can measure the change in the light intensity over time. The faster the intensity increases, the higher the aggregation will be (Shin et al. 2009). This quantified measurement of aggregation is generally called an aggregation index (AI); it is a unit-less number calculated in this case by finding the area under the curve (AUC) divided by the sum of AUC and the area above the curve (AAC) as seen in Figure 1. Therefore:

$$AI = \frac{AUC}{(AUC + AAC)} * 100 \qquad 2.$$

The light transmittance-time curve is integrated for 10s, starting at the minimum point of transmittance, where disaggregation ends (Simmonds et al. 2011).

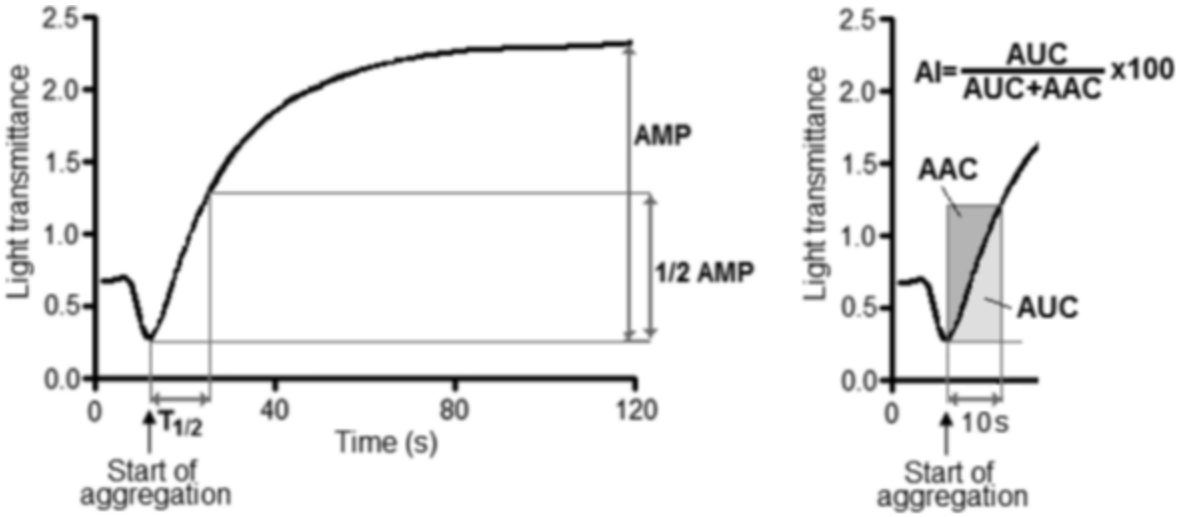

Figure 1 Calculation of aggregation index (Simmonds et al. 2011).

Figure 2 presents a typical result of light intensity vs. time measured by the aggregometer. Initially, the intensity quickly drops due to the disaggregation, then more slowly, increases. The aggregation index from the test represented here was 41.5, which is typical of normal, physiological conditions.

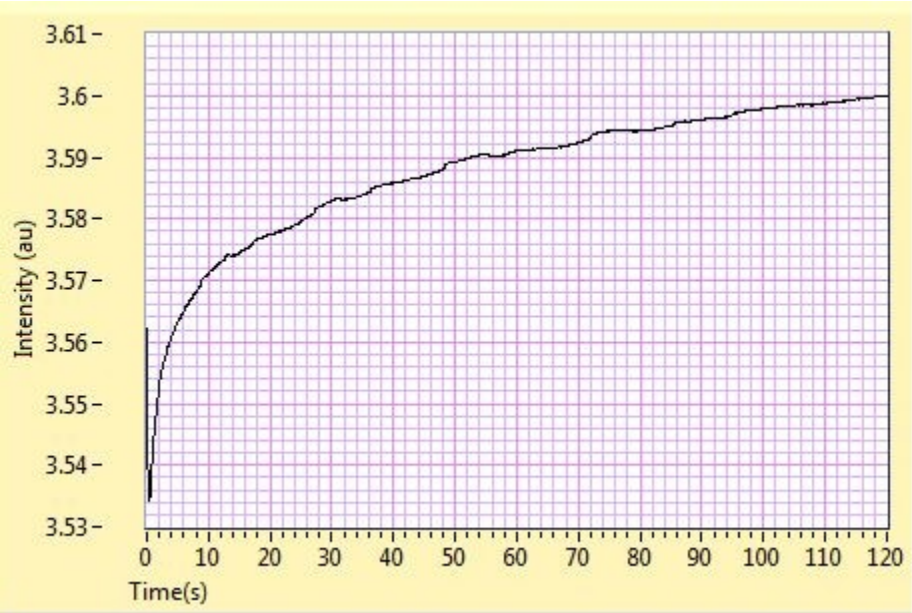

Figure 2 Result of test using aggregometer, showing light intensity over time.

2.2 Modification of aggregation properties: Dextran

Effects on aggregation

In addition to the proteins discussed above, other polymers and macromolecules can also effect aggregation when introduced into the blood. Dextran is an example of one such macromolecule. Dextran is a neutral polyglucose formed from a chain of glucose molecules that are linked in straight and branching patterns. Its molecular weight can vary greatly depending on how many glucose molecules are linked together, normally ranging from 2 to 2000 kDa. The aggregation change cause by dextran is a function of both its molecular weight and also its concentration when introduced to the RBCs. For example, dextran at 40 kDa, which is about the

lowest molecular weight dextran can have while still affecting aggregation, will inhibit RBC aggregation. Dextran with molecular weights of 60 to 2000 kDa, conversely, increase aggregation, with the strongest increases occurring in the range between 70 and 300 kDa (Nash et al. 2008).

Other macromolecules that can effect aggregation include polyethylene glycol (PEG), polyvinylpyrrolidone (PVP) and pyridine. The mechanisms by which these macromolecules increase or decrease aggregation are not yet fully understood. One explanation, however, is that, by the same mechanism behind the "depletion method" of rouleaux formation, the macromolecules increase the concentration of the surrounding plasma, thus lowering the relative concentration near the surface of the cellular membrane, and increasing the attractive forces between the RBCs (Baskurt et al. 2012).

2.3 Margination

Margination is defined as the movement of particles in a fluid flow toward the walls of the channel. In blood, these particles are principally white bloods cells, which need to migrate to the vessel wall in order to initiate much of their functions in the body.

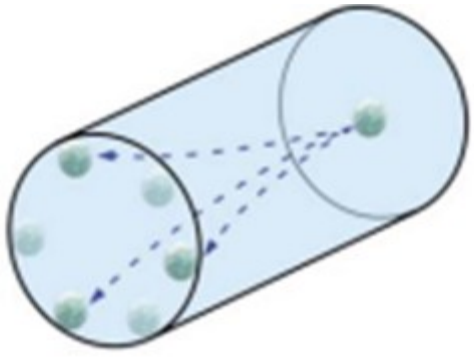

Figure 3 Particles marginating in a circular channel (Yang et al. 2011)

Cell free layer

When blood flows through small blood vessels, a layer free of red blood cells, called the cell free layer (CFL), forms near the wall. This occurs because red blood cells in the vessel migrate towards the center of the vessel in laminar flow. The mostly likely explanation for this phenomena is due to the deformability of the red blood cells, which can cause them to bounce off the walls of the channel and congregate in the center (Pan et al. 2011). The CFL separates the vessel wall from the central flow, which carries a greater concentration of the red blood cells – this central flow region is often called the RBC core. In areas of higher than normal shear rate, such as at a bifurcation (when a parent vessel braches into two daughter vessels) or at a site of constriction, the CFL will not form (Pan et al. 2011).

Physiological importance

Margination is important because it can influence how quickly a molecule in suspension in the blood can be absorbed by the body. If there is a greater movement of molecules towards the walls of a blood vessel, more of the molecule will be in contact with the wall of the vessel, where absorption takes place. Higher margination also means that more of the particles will enter smaller vessels (>100 μm) such as arteriole and capillaries that branch from larger ones, since the smaller vessels skim their contents from the peripheries of the mother vessels. This skimming results in lower hematocrits in the smaller branches of the vessel, a phenomenon known as the Fåhræus effect, and a higher concentration of the marginating particles. The capillaries are where the greatest transfer across the walls of the blood vessels occurs due to their very high surface area and the thinness of their vessel walls.

Leukocyte margination

White blood cells (leucocytes) show a great deal of margination in order to move to the walls of a vessel and adhere there (Freund 2007). For the WBC to do this, they have evolved

specialised adhesion molecules which can bind to receptors on the vessel wall allowing capture of the fast flowing WBCs (Nash et al. 2008). They marginate to sites of inflammation or infection in response to chemical signals sent off by the tissue located there.

Drug absorption

Drug-tissue interaction must occur at the walls of a blood vessel. Consequently, an increase in margination at a site requiring a specific drug action would increase the amount of medication available to the tissue at that site, relative to the rest of the body. In order to better understand and improve or tailor drug absorption, it is important to understand the physics of margination.

Adhesion as a measure of margination

While margination is defined as the lateral movement of particles toward the channel wall, it can be difficult to measure this lateral velocity of particles in a laboratory setting. Instead, adhesion is most often used as a measure of margination, as it is generally easier to measure the amount of particles that adhere to the walls after flowing blood though a vessel or channel. The amount of adhered particles measured can be used to infer the level of margination that occurred, as only particles that had marginated would be able to adhere to the walls. Higher relative amounts of adhered particles would therefore indicate a greater level of margination occurring (Apolito et al. 2015).

2.3.1 Factors that affect margination in analogous blood

Particle size

Many studies indicate that there is an optimal particle size for margination to occur, but there is no consensus on the exact size. Multiple studies suggested that spherical particles 500 nm and larger exhibited marginating behaviour, whereas particles 200 nm and smaller became

trapped between RBCs in the core of the blood flow, away from the channel walls. For particles larger than 500 nm in diameter, adhesion to the vessel walls was found to increase with the particle's size, as shown in Figure 4 (Charoenphol et al. 2010).

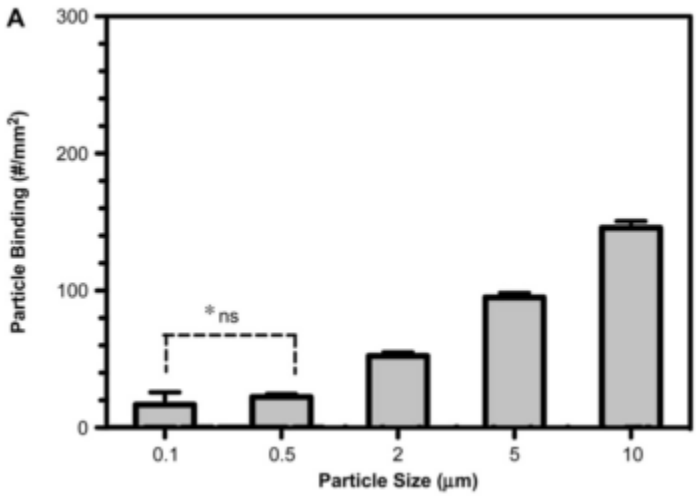

Figure 4 The effects of particle size on the number of particles binding the wall of a channel *ns = no significant difference (Charoenphol et al. 2010)

It was also found that as the radius of a particle decreases, the time taken for the particle to reach the wall greatly increases. When a particle approaches the wall, Van Der Waals forces begin to dominate and the particle experiences a "jump into contact" behaviour towards the wall (Decuzzi et al. 2005).

T.-R. Lee et al., (2013) found that particles larger than 100 nm would rapidly move from being randomly distributed throughout the vessel, past the cell free layer and into the boundary layer at the vessel wall. Particles 100 nm and smaller would stay randomly distributed and perform less margination. Also, in their study, spherical particles 2 µm in diameter were found to show disproportionately higher margination than nanospheres for all hemodynamic conditions evaluated. This was attributed to the poor ability of the nanospheres to localize to the wall region from midstream.

However, a different study by Toy et al., (2011) found that 65 nm liposomes deposited onto vessel walls at a higher rate than 100 nm liposomes, and 100 nm deposited at a higher rate than 130 nm liposomes, which contradicts the idea that particle less than 100 nm in size are entirely randomly distributed, and that at that scale, size may still play a role in aggregation.

Apolito et al., (2015) found that small spheres, 1µm in diameter, marginated significantly less than larger 3µm spheres, and that larger spheres were located a larger distance from the vessel's center-line, on average.

Particle shape

Non-spherical particles with higher aspect ratios have been found to marginate more readily than spherical particles. Particle rotation seems to be a key factor in aiding margination. (Gentile et al. 2008) found that the number of quasi-hemispherical silicon particles marginating towards the surface decreases with the shear rate τ following a power law τ^{-1}, regardless of their density and size. Also, the number of marginating spherical silica particles decreases with the shear rate according to the scaling law $\tau^{-0.63}$ and that the number of marginating discoidal polysilicon particles decreases with the shear rate according to the scaling law $\tau^{-0.85}$.

Toy et al (2011) found that gold rods (56 nm in diameter) marginated at a much higher rate than gold spheres (60 nm). Gold, however, has a much higher density than any biological material, so it is not known whether the same characteristics apply to physiological materials. Doshi et al., (2010) used 1µm, 3µm and 6µm spheres, as well as rods fabricated from spheres using the film-stretching method and, like Toy et al. (2011), found that rod-shaped particles had significantly higher adhesion compared to spherical particles. Another study (Apolito et al. 2015) compared margination propensities for spheres (1µm and 3µm), discoids (1µm x 400nm) and rods (400nm x 1.8µm). The rods experienced significantly lower levels of margination than either spheres or disks when at approximately the same size and density. This finding is

contradictory to what was found by Toy et al. (2011), but we note that the rods used by Apolito et al. (2015) were much larger. Apolito et al. (2015) also found no significant difference in margination between spheres and discoids.

Particle density

Studies are often too different to draw any meaningful conclusions on the general behaviour due to the different conditions used in different experiments (Nash et al. 2008). It has been shown, however, that particles having higher densities will marginate less than those with lower densities. This finding was found from studies using liposomes, iodinated liposomes, iron spheres and gold spheres (Toy et al. 2011); liposomes, as the least dense of these particles tested, marginated the most while gold spheres, as the most dense, marginated the least.

Particle stiffness

Conflicting simulation results have been reported for the effect of particle stiffness on the margination of particles and cells. In one study, it was found that RBC elasticity and deformability had no effect on the margination of WBCs (Freund 2007). Other studies, however, showed that heterogeneous collisions between a stiff and an elastic particle lead to increased margination (Kumar & Graham 2011).

Shear rate

The common use of particle adhesion to quantify the degree of margination leads to inconclusive results about the effect of varying shear rate on margination. Particles may become detached from the wall due to increasing hydrodynamic drag and/or due to collision with RBCs and so studying the effect of shear rate on particle margination has produced no conclusive results (Nash et al. 2008).

Aggregation

No consensus has been reached on the effects of RBC aggregation on margination of white blood cells and other microparticles in blood vessels. Several studies have examined the role aggregation plays, but have reported conflicting results (Carboni et al. 2014). Previous studies that have investigated the effects of aggregation have examined it in a Couette cylinder (Guilbert 2009) or with parallel plate flow chambers (Namdee et al. 2013). No study has yet examined aggregations effects in a circular channel.

2.4 *In vitro* model for micro vessels

To study blood flow *in vitro*, a vessel must be prepared for the blood to flow through. To study flows that occur in the small artery and capillary networks, these vessels are constructed at a micro-scale. Several aspects must be kept in mind when designing the vessel such as the cost of making each channel, reproducibility of the channel to ensure similarity, the time required for fabrication, how blood acts at the surface of the material used in the vessel, and the geometry of the channel and its complexity.

2.4.1 Introduction to photolithography

Lab-on-a-chip devices are widely used in the field of bio-fluid mechanics, and other microscale chemical analyses. Their reduced volume requirement and high definition features allow great control and a very large range of function, limited only by their design.

Photolithography is a technique using moulds, UV light and conformable photomasks to create two and three dimensional structures (Rogers & Nuzzo 2005). It is often used for its applications in biotechnology and has been expanding rapidly as a technique since the 1990's. There are several different types of photolithography which can range in complexity; however we are using one of the simpler methods because it sufficiently met the requirements of the experiment.

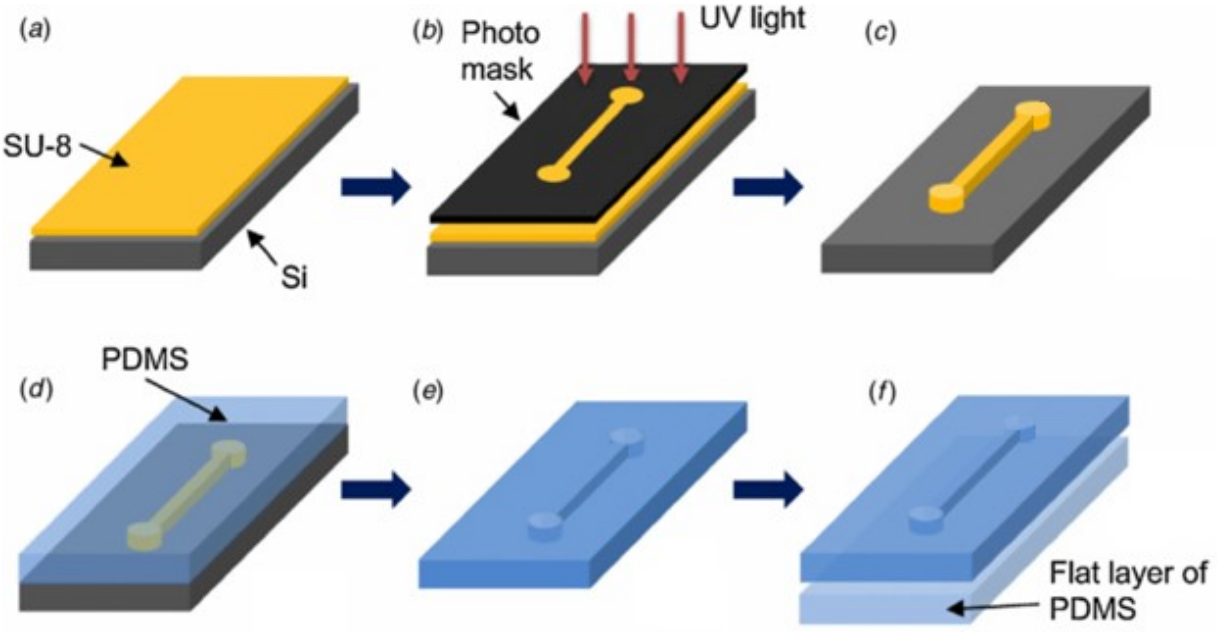

Figure 5 Simple, single-layer photolithography adapted from (J. Lee et al. 2013)

The general technique involves spin coating SU-8 onto a silicon wafer as seen in Figure 5: (a), then placing a photomask on top of the SU-8 photoresist. The holes in the photomask allows UV to pass through and cure the SU-8 were it hits (b). The non-cured SU-8 is dissolved off of the silicon wafer, leaving only the cured SU-8 acting as a master mould for future use (c). After the master mould is made, PDMS can then be poured onto it (d). The PDMS hardens and takes the negative shape of the mould and can then be removed from the mould (e). The hardened PDMS then has holes punched into the desired channel inlets and outlets. It is then bound to another completely flat layer of PDMS or glass using oxygen plasma, which binds the PDMS, enclosing the channels with a "fourth wall" so that liquids may flow through them (f).

In this simple method described above, only a single UV step is used. This limits this method by only being able to project a single two-dimensional image onto the SU-8 photoresist, and resulting in straight-walled channels. If more complicated designs are required, such as channels extending into three-dimensional space, many other steps are required.

Multi step photolithography

Other, more complicated techniques can involve many more steps in the process to fabricate the master mould. If multiple levels are desired, each with varying geometry, one may use additional photomasks and layers of photo-resist chemical to build on previous structures on the wafer using a position marker to align all the photomasks with the wafer. This procedure is illustrated in Figure 6.

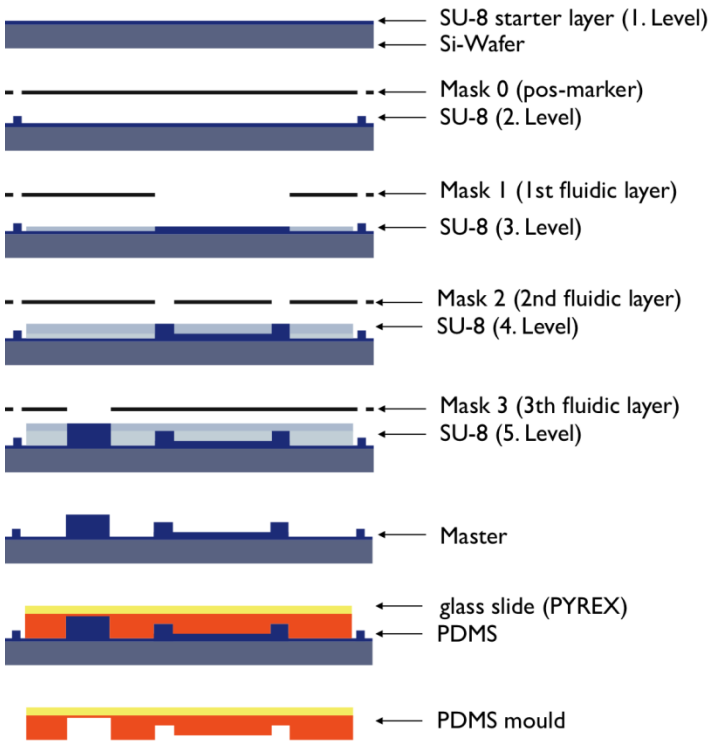

Figure 6 Multi-layer photolithography technique.

These previous examples would only produce straight walled edges because the photoresist and photomask are exposed to the UV light perpendicular to their surfaces; however, techniques can be used to create wells in material built onto the wafer to produce more rounded channel cross-sections. These techniques often involve etching the material with a strong solvent or acid (Betancourt & Brannon-peppas 2006).

2.4.2 Round channel fabrication methods

Methods to create a rounded wafer masters exist, however they can only create a semicircular shape. Two moulds of PDMS would therefore be required, which must then be mated using an aligner to connect the two halves to create the full circular channel. One method to do this uses a positive photoresist and a clear-field photomask, exposing everything on the wafer, except the channel to UV (San-miguel & Lu 2013). As shown in Figure 7, unlike most negative photoresists, when the positive photoresist is baked at a sufficiently high temperature, the positive photoresist will reflow; therefore, the initially rectangular channel will gain rounded sides. In order to make a fully round channel with this method, two moulds must be poured onto the silicon master and then, using an aligner, the two moulds would be bonded to together forming a round channel from the half-elliptical ones. This process must be very precise in order to properly align the two moulds.

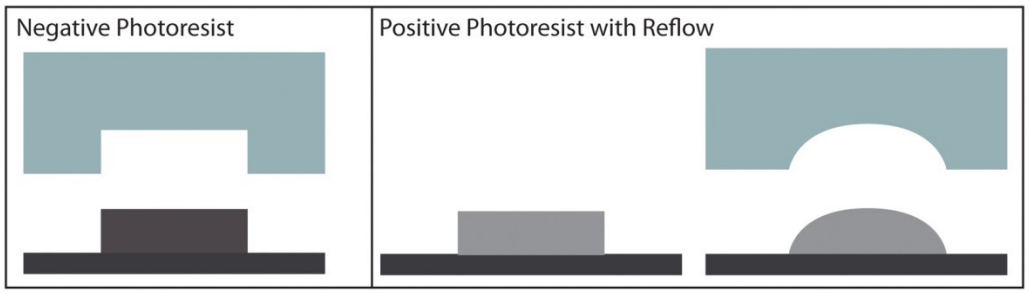

Figure 7 Example of using reflow with positive photoresist to create a half elliptical channel (San-miguel & Lu 2013)

Other methods can be used to make circular PDMS channels. These methods do not require additional modifications to be done to the silicon wafer and are discussed in the following sections. There are three main methods to do this: the Air Pressure, Wire, and Glass Capillary methods.

Air Pressure

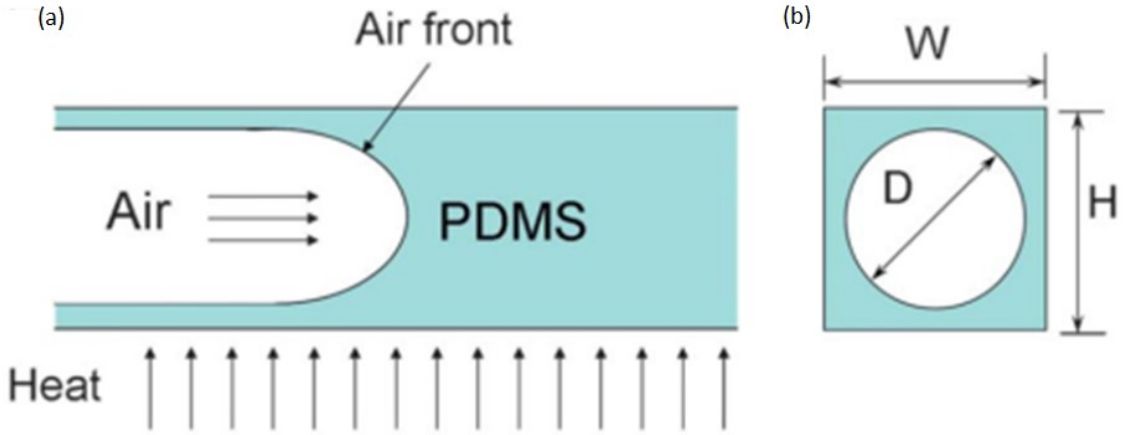

Figure 8 Diagram of air pressure creating a circular cross section in liquid PDMS (Abdelgawad et al. 2010)

The air Pressure method starts off using normally made rectangular or square channels in PDMS. Once the channel is formed, liquid PDMS is injected through one of the inlets, filling the channel. After the channel is filled, air is blown through the channel, applying pressure to the injected PDMS (Figure 8 a). The air pressure forces a central, circular channel to be formed inside the rectangular one, with all the liquid PDMS pushed to the sides or out of the channel by the pressure (Figure 8 b). This method is inexpensive and effective; however not all the channels made will be exactly the same - since the air pressure required to form the round section, or the viscosity of the PDMS would be slightly different, the diameter of the channels will not all be identical (Abdelgawad, Chien, et al. 2010).

Wire Method

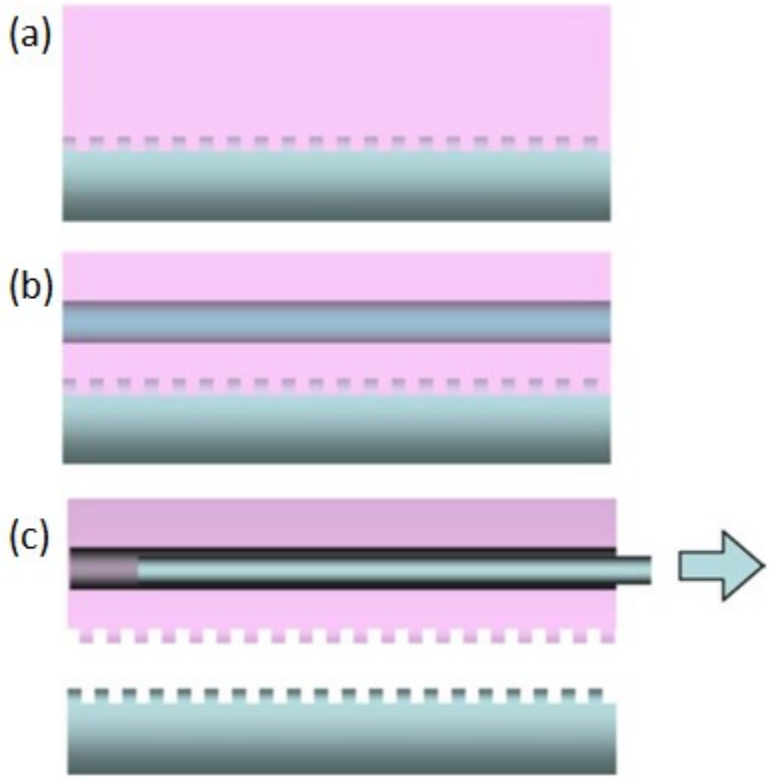

Figure 9 Diagram of wire method to create circular microchannels (Perry et al. 2007)**.**

In the wire method, a smooth metal wire running through the rectangular channel is suspended between two supports, and PDMS is poured around it as shown in Figure 9 (a-b). After the PDMS has cooled, the wire is extracted (c), leaving round channels in the PDMS. These channels are identical to others made with the same wire. Using this method, however, is more complicated, since the wire doesn't leave easily accessible inlets and outlets, because the wire will often be 50-100 µm in diameter, therefore the inlets and outlets would also be 50-100 um in diameter - too small to attach tubing to. The inlets and outlets must therefore be added after the channel has been formed. This is often done by attaching separately fabricated PDMS end pieces to both sides of the channel. These end pieces seal off the entrances to the channels formed by the wire and can create a connection to the round channel with a larger access. An

additional concern is that during the removal of the wire from the PDMS, the PDMS touching the wire can often get torn, creating blockages and ruining the channel.

Glass Capillary

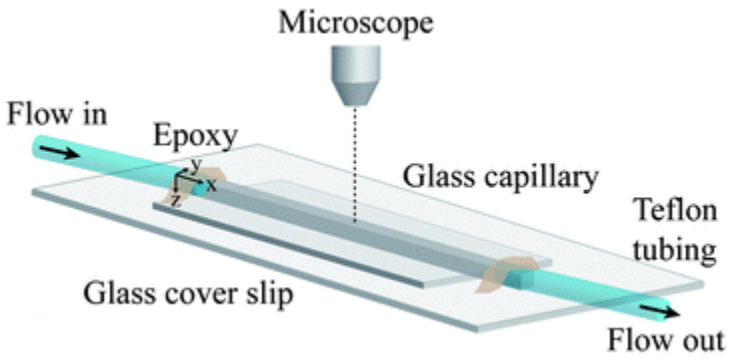

Figure 10 Diagram of a glass capillary tube being used as a circular channel (Pandey & Conrad 2012)

Glass Capillary is the simplest method to create a circular channel. A glass capillary tube matching the desired diameter forms the channel and plastic or Teflon tubing can be attached to either end, forming the inlet and outlet (Figure 10). One problem with this method, however, is that red blood cells can interact and adhere to the glass and result in abnormally high levels of hemolysis which may interfere with the experiment (Fenn 1921).

2.4.3 Flow in microchannels

In microfluidics research, rectangular vessels are much more easily fabricated than round vessels, due to how the cheaper fabrication processes work, such as PDMS fabrication. Round vessels, however, have very different rheological properties than rectangular ones. For example, the Hagen–Poiseuille flow and velocity profile equations for rectangular (as seen in Figure 11) flow are (Bruus, 2006):

$$Q_{rec} \approx \frac{h^3 w \Delta p}{12 \eta L}\left(1 - 0.630\frac{h}{w}\right) \quad (3.)$$

and

$$v_{x_{rec}}(y,z) \approx \frac{4h^2 \Delta p}{\pi^3 \mu L}\sum_{n,odd}^{\infty}\frac{1}{n^3}\left(1 - \frac{\cosh\left(n\pi\frac{y}{h}\right)}{\cosh\left(n\pi\frac{w}{2h}\right)}\right)\sin\left(n\pi\frac{z}{h}\right) \quad (4.)$$

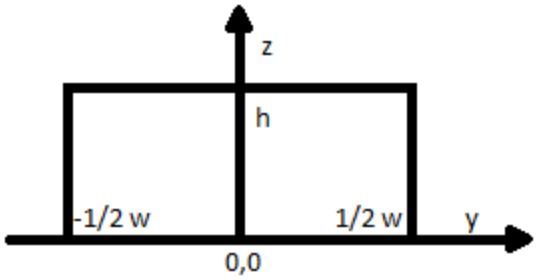

Figure 11 Diagram of a rectangular cross section of a channel w is width of the channel, h is height of the channel

On the other hand, the equations for flow in a circular, or ovoid cross-section (as seen in Figure 12) are (Bruus, 2006):

$$Q_{circ} = \frac{\pi \Delta p}{4\mu L}\frac{a^3 b^3}{a^2 + b^2} \quad (5.)$$

and

$$v_{x_{circ}}(y,z) = \frac{\Delta p}{2\mu L}\frac{a^2 b^2}{a^2 + b^2}\left(1 - \frac{y^2}{a^2} - \frac{z^2}{b^2}\right) \quad (6.)$$

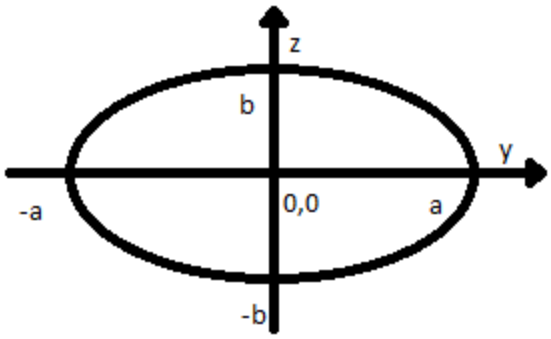

Figure 12 Diagram of an ovoid cross section of a channel a is radius1 of the channel, b is radius2 of the channel

Also, the velocity profiles of the particle's flow through the vessels are very different, as shown in Figure 13.

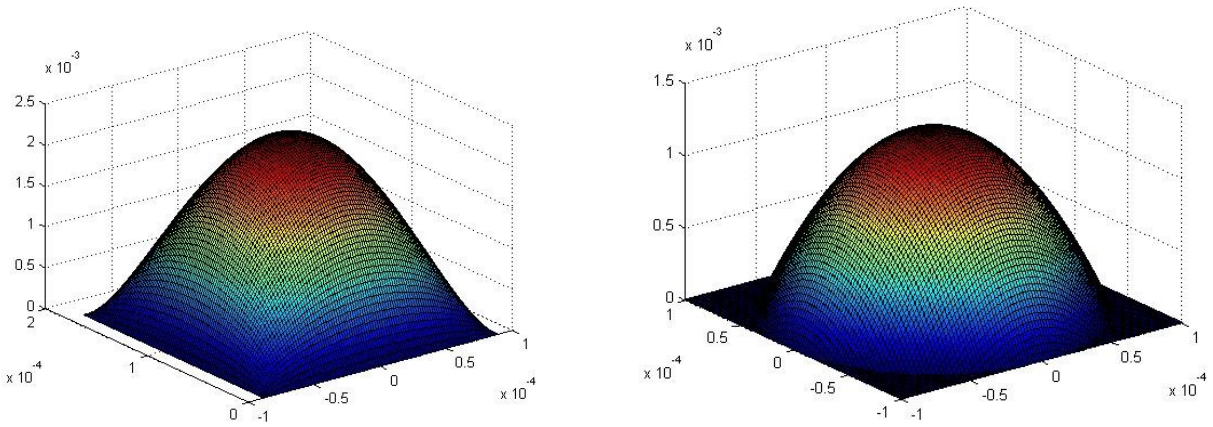

Figure 13 Velocity profiles in different channel geometries: Square on the left and circular on the right.

Shear stress is also dependent on the channel geometry as it is directly related to the shear rate, which, in turn, is directly dependent on the flow rate. Therefore, due to the differences in the velocity distributions between rectangular and circular channels, the shear stress are very different as well.

2.5 Conclusion

No consensus has yet been reached on the effects of aggregation on margination of white blood cells and other microparticles in blood vessels. Several studies have examined the role aggregation plays, but have reported conflicting results.

Rectangular channels have four vertices that are equidistant from the center of the channel. Consequently, the creation of the cell free layer in a rectangular channel would be focused on those points, as shown in Figure 14 (c), and particle margination would be strongest towards those points (Yang et al. 2011). Comparatively, the axisymmetric walls of circular channels allow the formation of a more steady and smooth cell free layer. Therefore, in order for the results to be more physiologically accurate, circular microchannels must be developed that can be used for the experiments.

The primary objective of this thesis is to test the effects of aggregation on the margination of microparticles in circular microchannels. To meet this objective, the Air Pressure method was chosen because it is the most easily modifiable method and, given that the experiment aims at examining particle margination, or particle movement to a vessel's wall, the fabricated channels must be modified in a way that will aid us in examining the level of margination in the channel.

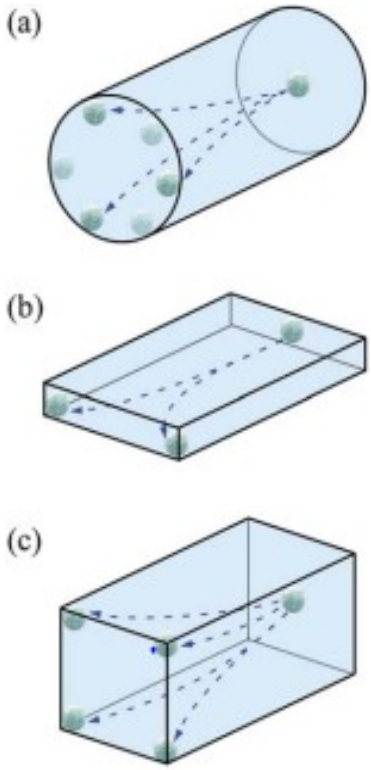

Figure 14 Particle margination in different microchannel cross-sectional shapes (Yang et al. 2011)

3 Design of biomimetic microvascular channels

This chapter will address the first and second objectives of this thesis, that are (1) to design and fabricate a round channel in PDMS and (2) to develop a method to capture and count the particles that migrate to the wall. Meeting these objectives will involve the following steps:

1. designing a photomask for the procedure,
2. optimizing the photolithography and channel rounding procedures,
3. identifying biochemical coatings to bind the particles to the channel walls, and
4. fabricating the final product: the round, treated channels for use in the final experiment, in which we examine the effects of aggregation on the margination of microparticles in human blood flow.

3.1 Photomask design

In the photolithography process, the photomask is the blueprint that prescribes the final geometry of the microchannels. The desired channel pattern is printed on the photomask. It is placed on top of the layer of photoresist that coats a silicon wafer, which is then exposed to light. The photoresist will cure at all of the locations corresponding to the light regions on the mask that let light through, but not under the dark regions. The photomask allows for very accurate and highly reproducible patterning of the wafers.

The photomask was designed in Solidworks for a 4-inch diameter silicon wafer. The digital design was then sent to CAD/Art Services, Inc. (Bandon, OR), where it was printed onto a clear cellulose acetate sheet as a high precision photomask. The photomask shown in Figure 15 is the photomask used for all tests; it has ten channels, all 100 μm in width. There were five different channel lengths, two each of 1 cm, 2 cm, 3 cm, 4 cm, and 5 cm.

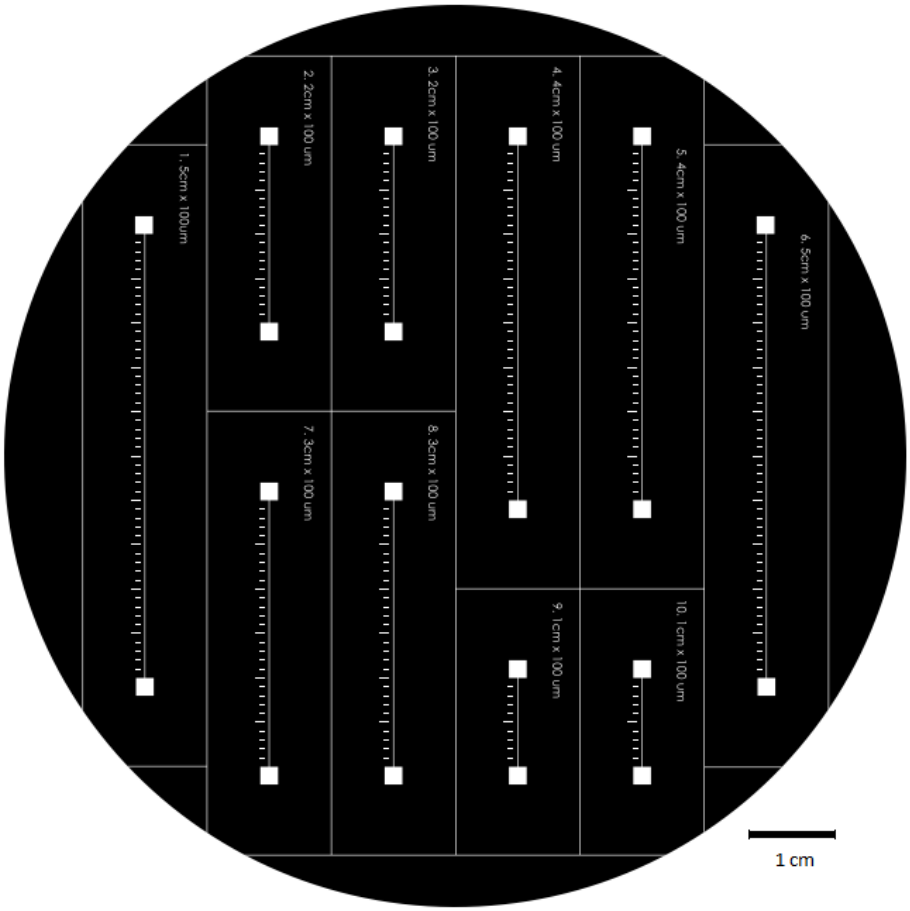

Figure 15 Photomask used for wafer fabrication

3.2 Wafer fabrication: standard procedure

3.2.1 Fabrication method

Originally, a standard procedure was used to fabricate the wafer mould for square channels (MicroChem, Product information), which is outlined in the following.

The silicon wafer was cleaned to remove a naturally occurring silicon oxide formation that results from exposure of the wafer to oxygen in the air. To clean the wafer, it was immersed in a 1% v/v hydrofluoric acid (HF) solution (R38161001A: Fisher Scientific, Nepean, Canada). The HF solution dissolves the oxide layer making the surface much more hydrophobic, and thus improves bonding with the SU-8 50 Photoresist (Y131269: MicroChem, Westborough, USA).

After the wafer was cleaned, photoresist (SU-8) was spun onto the wafer using a spin coater (WS-650-23B: Laurell Technologies Corporation, North Wales, USA) to evenly distribute the layer of the SU-8 over the wafer's surface. The wafer was spun at 500 rpm for 30 seconds to first spread the photoresist over the wafer, and then at 1000 rpm for 30 seconds to obtain a final thickness of 100 µm. The reason this thickness was chosen was so the final channel would have the dimensions of 100 µm x 100 µm, which would keep the channel in the physiological range of small arteries, where margination plays an important role in the body. The speeds and duration of the spin cycles were taken from a graph provided with the SU-8 product. To solidify the newly applied SU-8 coating, the wafer was exposed to two baking steps: the first one being a soft bake at 65°C for 10 minutes, which was followed by a hard bake at 95°C for 30 minutes. The photomask (Figure 15) was then mounted to the wafer, on top of the photoresist, and the wafer assembly was placed in a UV box (Intelli-Ray 600W: UVitron International, West Springfield, USA) and subjected to UV exposure for 2 seconds, delivering a total light intensity of 350 mJ/cm^2. The UV light passed through the negative space in the photomask curing only the elements that were exposed, and in this case creating solid structures on the wafer. The wafer then went through another two baking steps: a soft bake at 65°C for 3 minutes and then a hard bake 95°C for 10 minutes, in order the fully cure the UV exposed sections of the SU-8. The wafer was finally immersed in a SU-8 developer solution (Y020100: MicroChem) for 10-15 minutes until all the non-cured SU-8 was dissolved from the wafer, leaving only the cured sections.

3.2.2 Measuring the Quality of Wafers and Channels

The quality of the wafer that was prepared was then assessed by pouring the PDMS over it to create a negative copy, and then cutting a thin cross-sectional piece from the cured PDMS

and examining it under a bright field microscope at the location where the PDMS was moulded by the wafer. The cross-sectional piece was then measured, using an image captured though a bright field microscope, at the width of the channel at its widest point (most often the top of the channel), and at its narrowest point (most often the bottom of the channel). The height of the channel and the angle of the walls connecting the top and the bottom were also measured.

The average width and the height were compared, and the channels which had the least disparity between those two measurements were deemed superior to those which had a greater disparity.

3.2.3 Channel quality

Based on their measurements, the results from the first multiple fabrications of wafers were not ideal.

Wafer 1: Wafer 2:

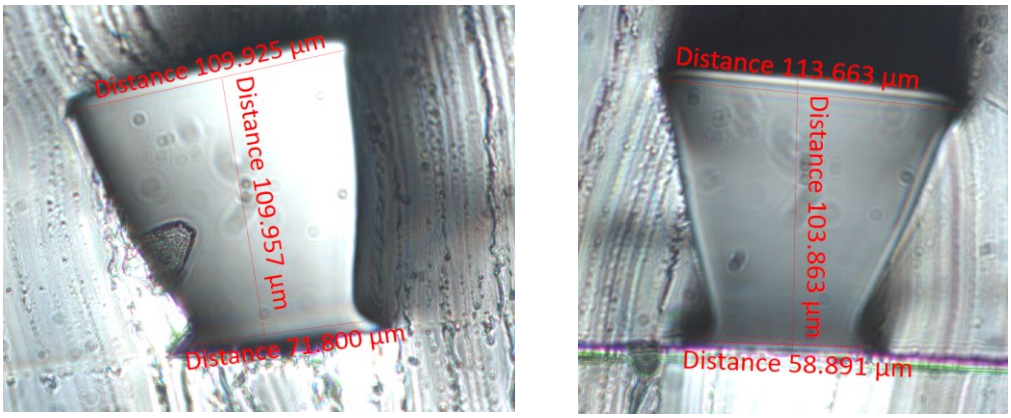

Figure 16 Dimensions of the first test of fabricating wafers using photolithography: Left (top width: 110, bottom width: 72, height: 110) right (top width: 114, bottom width: 59, height: 104)

As shown in Figure 16, the PDMS channels that were cured on the master wafers were far from the 100x100µm perfectly square cross-sections desired: the base of the wall formed from the cured SU-8 is approximately half the width of the top and the top wall of the channel is

not parallel with the bottom. Additionally, not shown here, some structures lifted off from the wafer and stuck to the PDMS after it was poured, indicating that the developed SU-8 had not properly annealed to the wafer. To correct for these imperfections, the original procedure was modified in attempts to improve the final channel quality. The manner in which we optimized the procedure is described in the following section.

3.3 Optimisation of the photolithography methods

Previous studies have examined how slanted walls are formed in photolithography, as well as how improper annealing of the SU-8 to the wafer can occur (Krogh 2003). We used the results of these studies, along with recommendations from a photolithography troubleshooting guide (MicroChem 2012) to introduce changes to the procedure, which were then systematically evaluated.

After etching the wafer with HF and washing it with water, a baking step was used to ensure that the wafer was completely dried. This may help increase the chance that the SU-8 properly sticks to the wafer and doesn't lift off after processing. (MicroChem 2012).

Relaxation time can be added after spin coating to allow the SU-8 to level out more evenly. This would help prevent any wavy pattern that might emerge and help the annealing of the SU-8 to the wafer (Krogh 2003).

3.3.1 Identification of possible changes to improve the product

Five different steps were identified that could be added to or modified in the original procedure in order to improve it. Each one was tested separately, using a whole wafer. They are:

1. Additional step to bake at 120°C for 10 minutes after HF etching, prior to adding the SU-8 in order to ensure that the wafer is completely dried after washing. (Krogh 2003)

2. Modification of a step to bake for 100 minutes at 95°C (one minute for every μm thickness) during the first soft baking step, instead of 30 minutes (MicroChem 2012)
3. Additional step to allow 10 minutes of relaxation time after the first hard bake and 10 minutes after UV exposure (MicroChem 2012).
4. Additional step coating the SU-8 with glycerol to ensure that the photomask is positioned as close as possible to the SU-8 coating, eliminating any air gaps between them and reducing light diffraction through the air after UV passes through the photomask (Pinto et al. 2014).
5. Modification of a step to using a 4 second UV exposure time instead of 2 seconds to hopefully create walls that are straighter (Martinez-duarte 2014).

3.3.2 Results of the Optimization Process

Table 1 Changes made to original photolithography technique

Change made to procedure	Result	Dimensions
No change (original procedure)	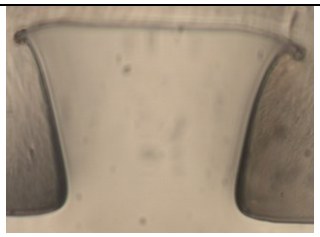	Top Width: 171 µm Base Width: 117 µm Height: 104 µm Q= 53.3
1) Bake at 120°C for 10 minutes after HF etching (Krogh 2003)	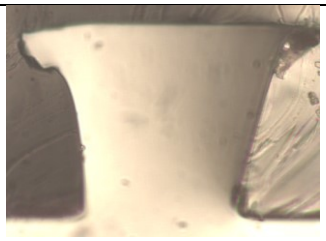	Top Width:146 µm Base Width: 89 µm Height: 118 µm Q= 25.6
2) Baked for 100 minutes at 95°C, after spin coating (MicroChem 2012).	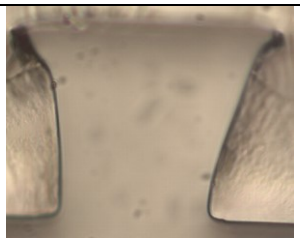	Top Width: 141 µm Base Width: 81 µm Height:104 µm Q= 20.4
3) 10 minutes relaxation time after 1st hard bake and 10 minutes after UV. (MicroChem 2012)	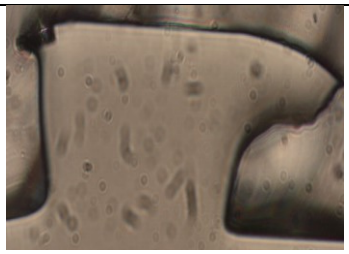	Top Width: 241 µm Base Width: 141 µm Height: 100 µm Q= 215.6
4) Glycerol coating. (Pinto et al. 2014)	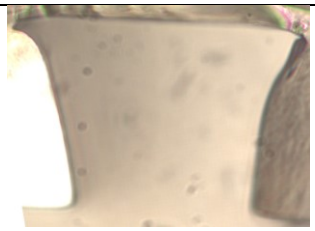	Top Width: 143 µm Base Width: 91 µm Height: 106 µm Q= 19.3
5) 4 second UV exposure time. (Martinez-duarte 2014)	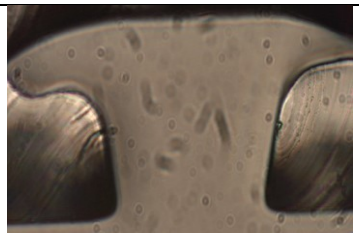	Top Width: 254 µm Base Width: 105 µm Height: 105 µm Q= 237.1

Each change was performed on one full wafer and the channels were measured as was done previously. A measure of the square-ness of the channel was added, to assess the channel quality. Channel quality Q was calculated using only the measurements of the widths at the top and at the base of the channel because the height of the channel is a function of only the spinning speed during the spin coating step of the fabrication process, and not a result of any changes made to the procedure. The Q score is only to give us an idea of the square-ness of the channel, and to allow us to easily compare different channels, since, due to the further modifications of the channel to make it circular, a perfect square is not necessary, as the corners would be filled in by the injected PDMS. A Q of 0 would be ideal, with an expected width being 100 µm.

$$Q = \frac{(|Expected\ Width - Top\ Width|^2 + |Expected\ Width - Base\ Width|^2)}{Expected\ Width} \qquad 7.$$

Most tests returned results that were as bad as, or even worse than the original. The "T-shaped" tops of the wafers resulting from many tests are often indicative of over-exposure to UV light (MicroChem 2012). The channel that returned the best result was the test with the addition of glycerol on top of the SU-8 before UV exposure, with a Q score or 19.3.

3.3.3 Selected process modification

The step that was evaluated to produce the best result and was added to the original procedure was step number 4: a layer of glycerol was applied to the photomask before placing it on the SU-8 coated silicon wafer. This effectively ensured that the photomask was placed as close as possible to the SU-8 coating, with no air gaps in between. The glycerol also ensured that the UV cured the SU-8 evenly, reducing any diffraction of the UV light, giving the walls more perpendicular sides. The SU-8 also better adhered to the silicon wafer with this change, since less of it lifted off after curing PDMS on the silicon wafer.

3.4 Round channel fabrication and optimisation

Now that we have a method to fabricate rectangular channels, a procedure must be developed to let the channels have a circular cross-section and to capture the microparticles that will be flowed through the channel. To make the channels circular, Abdelgawad *et al.*'s 2010 air pressure method (from Section 2.4.2) will be used. However, the method will still need to be combined with another method to capture the microparticles.

3.4.1 Capturing particles in microchannels

To capture the particles that flow through the channels, two bio-molecules will be used: streptavidin and biotin. The microparticles used will come coated with streptavidin and the walls of the channel will be coated with biotin. Streptavidin and biotin have a very high binding affinity, so when a streptavidin coated particle touches the biotin coated inner wall of the channel during its margination, the particle will remain trapped there and can be imaged later for viewing and analysis (Huang, Wu, Kim, B. K. Kobilka, et al. 2006).

3.4.2 Biotin functionalization and circular channel fabrication

Due to the capturing method being used, the inner surface of the circular channel needed to be coated and functionalized with biotin groups (i.e. biotinylated) to immobilize the streptavidin coated fluorescent microparticles in the channel. To biotinylate the inner surface of the channel, we began with the method outlined by (Huang, Wu, Kim, K. Kobilka, et al. 2006). They premixed liquid PDMS pre-polymer with biotin molecules that were already bound to a phospholipid. A phospholipid has two sections: a long hydrophobic tail, which can be used to attach it to the PDMS matrix and a hydrophilic region, which attaches the phospholipid to the biotin. The hydrophobic tail embeds the molecule into the PDMS, which is also hydrophobic, placing the hydrophilic region and biotin group on the surface of the PDMS wall of the channel,

where it is exposed to the streptavidin coated particles that will eventually be flowed through the channel. The phospholipid chosen for the experiment was: 1,2-dioleoyl-sn-glycero-3-phosphoethanolamineN-(biotinyl) (870282C: Avanti Polar Lipids, Alabaster, USA) (Figure 17 A).

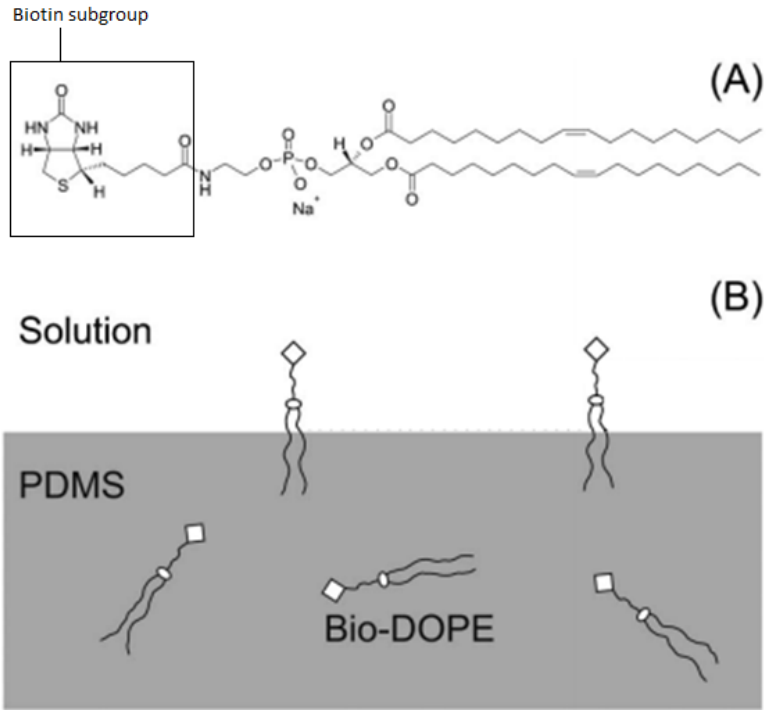

Figure 17 Biotynilated phospholipids used to biotynilate PDMS (A) chemical structure of 1,2-dioleoyl-sn-glycero-3-phosphoethanolamineN-(biotinyl) and (B) its integration into PDMS (Huang, Wu, Kim, B. K. Kobilka, et al. 2006)

Huang *et al.* 2006 used 10 µL of a 5 mg/mL phospholipid–chloroform solution added to 1 g of a PDMS pre-polymer and curing agent/hexane solution. They combined and degassed the mixture, then poured and spin coated it onto a silicon wafer. Once cured, this mixture resulted in biotinylated PDMS; however, Huang *et al.* 2006 only used this method to coat a silicon wafer with PDMS (Figure 17 B) to produce square channels. For our purposes, this method needed to be adapted to create round channels.

The method used previously by Abdelgawad et al. (2010) was used to create round channels in PDMS using air pressure. With this method the PDMS pre-polymer and curing agent were mixed at a 10:1 ratio, degassed and poured onto a master mould silicon wafer. The PDMS was then peeled off and inlet and outlets were punched into the PDMS. The PDMS from the wafer and another, completely flat piece of PDMS were then treated by oxygen plasma; after 30 seconds of plasma treatment they were pressed together and baked, forming an enclosed rectangular channel. To create the circular cross-sections, the rectangular channels were filled with liquid PDMS. The channel was then baked on a hot plate and compressed air with a constant pressure was forced through the filled channels for two minutes. After that, the channel was left on the hot plate at 100°C for another five minutes to ensure that the PDMS filling was thoroughly baked. These steps are illustrated in Figure 18.

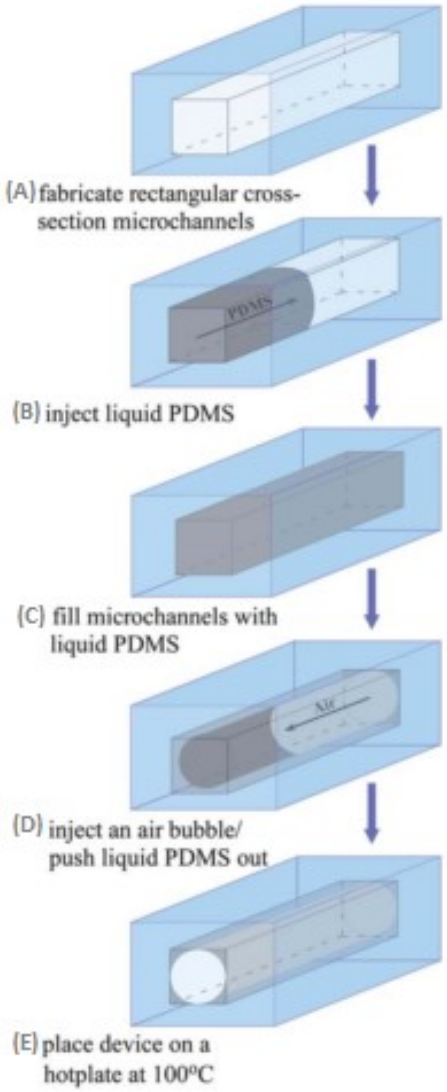

Figure 18 Steps in creating a round channel in PDMS (Yang et al. 2011)**.**

Another reason the air pressure method was chosen is because it can be used to easily coat the inner layer of the channels with biotinylated PDMS while forming the channel circular, allowing the two methods to be easily combined. The first attempt at combining and replicating both Huang *et al.*'s 2006 method to biotinylate PDMS and Abdelgawad *et al.*'s 2010 method to create circular channels from rectangular channels began with making a rectangular channel as was done in the earlier procedure. A silicon wafer was fabricated using the method previously

described in Section 3.3. The master mould had a raised area with the dimensions of 1.00 cm long by 106 µm high by 116 µm wide.

PDMS (without biotin) was poured over the channels and cured (Figure 18 A). The individual channels were excised after they had solidified and the PDMS chip was bonded to another, flat piece of PDMS using oxygen plasma treatment. The filling used to coat the insides of the channel was made using one gram of PDMS pre-polymer and curing agent that were mixed at a 10:1 ratio, and adding 10 µL of a 5 mg/mL 1,2-dioleoyl-sn-glycero-3-phosphoethanolamineN-(biotinyl) – chloroform solution (Figure 18 B-C). The filling was then injected into the rectangular channel and the channel was placed on a hot plate set to 100°C. Compressed air was injected into the channel using a pressure control device (MFCS^{TM}-EZ: Fluigent, Villejuif, France) at a constant pressure of 345 millibar for two minutes (Figure 18 D). The channel was then left on the hot plate at 100°C for an additional five minutes to ensure that the PDMS – biotinylated phospholipid filling was thoroughly baked (Figure 18 E).

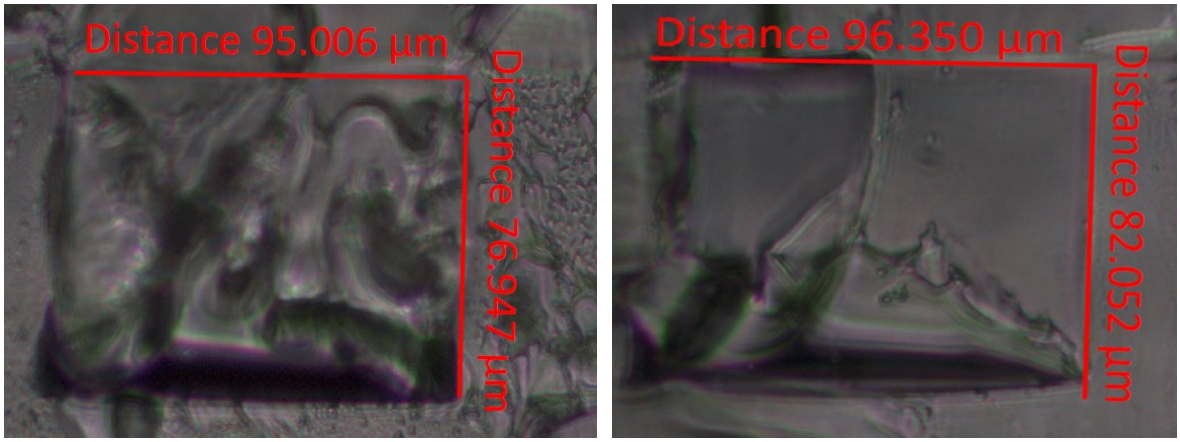

Figure 19 Filled channels after first attempt using the air pressure method

The results of these initial tests, as illustrated in Figure 19, were very poor. The filling was not completely cured after the baking process and, consequently, the filling in the channels did not form a circular cross-section: instead, it pooled in the channels, completely blocking

them once the air pressure was removed. To prevent this from occurring in the subsequent tests, the time that the compressed air pressure was applied to the filling while the channel on the hot plate was increased to 20 minutes to ensure that the filling stayed in place during the curing process. This increase produced the desired effect as will be shown in the following section.

3.5 Final method for circular channel fabrication

The final procedure, which adapted earlier methods to meet the specific requirements of this study, is outlined as follows: After the fabrication of the wafer mould (channel master) as outlined in Section 3.2, PDMS pre-polymer and a curing agent were mixed together at a ratio of 10:1. The mixture was degassed in a vacuum chamber (400-3910: Barnant Company, Barrington, USA), which created a maximum continuous vacuum environment of 72kPa, for one hour. The degassed mixture was then poured onto the channel master (made using the photomask shown in Figure 15), which was then placed in a glass Petri dish and baked on a hot plate for 30 min at 135°C. After the cured PDMS channels cooled down, they were peeled from the SU-8 master. The large piece of PDMS was then cut into the individual channel and reservoir holes were punched through at both the inlet and outlets. The casted PDMS section was then bonded to another flat piece of PDMS using an Oxygen Plasma etcher (PE-50: Plasma Etch Inc., Carson City, USA): the PDMS pieces were treated with oxygen plasma for 60 seconds, then were removed from the plasma etcher, pressed together, and baked on a hot plate for 5 minutes at 95C. To create circular cross sections, the square PDMS microchannels were filled with liquid PDMS made using the same ratio of PDMS pre-polymer and curing agent as was used before (10:1). 1 mL of this PDMS mixture was combined with 7.5 µL of a 5 mg/mL phospholipid–chloroform solution in a 1.5 mL microcentrifuge tube, mixed and then transferred to a syringe which was

connected to one inlet on the channel. The syringe was then used to fill the channel with the mixture.

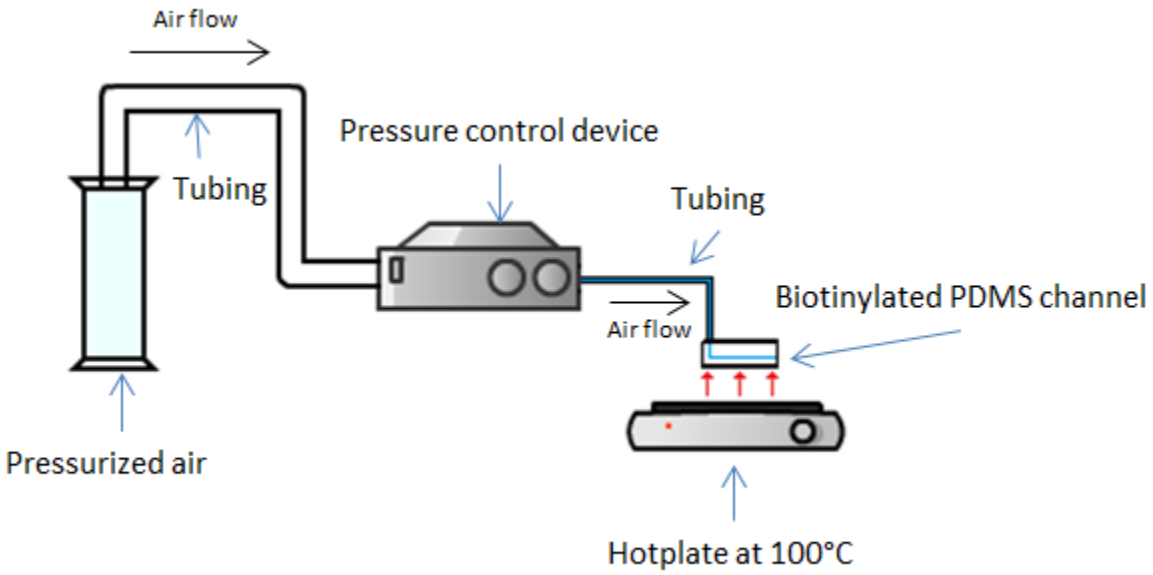

Figure 20 Diagram of air pressure set-up used to create circular channels. Pressurized air first leaves its storage and flows into the pressure control device, which ejects air at a controlled pressure of 5psi per cm of channel length. The controlled air flows into the channel while it is heated at 100°C and pushes the already inserted liquid biotinylated PDMS out to make a circular channel

As illustrated in Figure 20, a stream of compressed air (5 psi/cm) was injected through the PDMS-biotinylated phospholipid filled microchannels, while curing on a hot plate at 100°C for 20 minutes. In order to fully cure the deposited PDMS coating, the channel was then cured for another 20 minutes at 100°C with no compressed airflow.

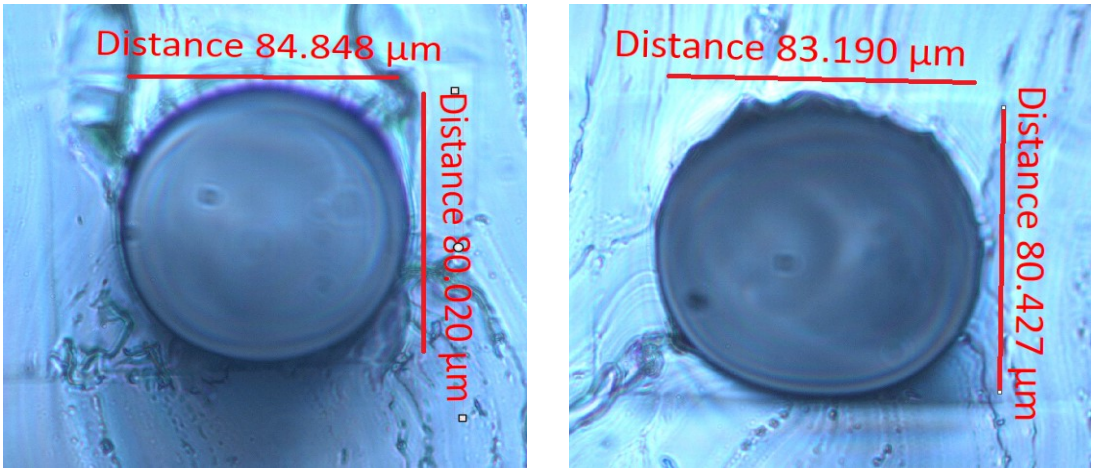

Figure 21 Circular channel formation

Results for Circular channel fabrication

Over 50% of the channels that were made using this procedure had near-circular cross-sections (Figure 21), as judged by the measurements obtained from images taken by a bright field microscope of the channel's vertical and horizontal diameters. The average diameter was 80 micrometers. This was considered to be an acceptable result, given that individual channels could be tested to ensure that they were circular prior to being used for the main experiments.

4 Effects of RBC aggregation on microparticle margination

With the round channels fabricated and a method that will be used to capture the particles prepared, as outlined in Chapter 3, we now need to devise a method to study the effects aggregation has on the margination of microparticles in the prepared channels.

4.1 Material and methods

4.1.1 Blood preparation

The whole blood used for all experiments was collected from volunteers by Gamma Dynacare laboratories (Ethics reference number: H11-13-06). We separated blood by centrifugation into three distinct layers. The plasma made up the top layer and had the appearance of a clear yellow liquid. This layer occupied approximately 55% of the total volume. The thrombocytes and leukocytes formed a second layer below the plasma called the buffy coat; it appeared as an opaque white thin layer occupying >1% of the total volume. Red blood cells formed the bottom, third layer, appearing as a thick, opaque dark red liquid occupying approximately 45% of the total volume. After cleaning the blood, samples could be prepared, having any desired hematocrit, simply by adding the desired proportion of clean RBCs to a suspension media of the researcher's choosing. A standard procedure for blood separation was used: the blood tubes were centrifuged at 3000 rpm for 10 minutes, then the plasma and the buffy coat were extracted and discarded and then phosphate buffered saline (PBS) was added to the remaining red blood cells to wash them. The RBC/PBS mixture was centrifuged again for another 10 minutes at 3000 rpm. The separated PBS was then removed and this washing step was repeated again for a final time. The RBCs were then transferred from the original tube into a sterile new one to await use.

Making autologous plasma

A mixture in which to suspend the RBCs was prepared for us to control the level of aggregation for the experiment, which could not be done using whole blood. First, Optiprep™ Density Gradient Medium (MFCD00867965: Sigma-Aldrich, St. Louis, USA) and PBS were combined at a ratio of 27% v/v of Optiprep™ to PBS. Optiprep™ was used to increase the density of the PBS, so that it would be similar to the density of RBCs in order to prevent sedimentation during the experiment.

Dextran

From the Optiprep™/PBS mixture, five different solutions were prepared, each having different concentrations of Dextran 500 (AAJ63702-22: VWR International, Radnor, USA): 0%, 0.5%, 1.0%, 1.5% and 2.0% w/v of the final solution, which was calculated from the volume of the Optiprep™/PBS preparation + 10%, from eventual addition of the RBCs at 10% hematocrit. Each solution was prepared in a separate 1.5 ml Fisherbrand™ microcentrifuge tube. The dextran was added to change the level of aggregation of the final preparation; the concentrations 1.5% and 2.0% were expected to result in equal to or higher than normal physiological levels of aggregation, whereas the 0%, 0.5% and 1.0% concentrations were expected to result in lower than normal levels of aggregation. Concentrations of dextran between 1% and 1.5% were expected to result in levels of aggregation equivalent to physiological levels, depending on the patient.

Red blood cells

After the dextran 500, Optiprep™, and PBS solution of autologous plasma was prepared, a volume of RBCs was added to the autologous plasma to achieve the desired hematocrit, which, for the present study, was 10%.

Fluorescent particles

Fluorescent particles coated with streptavidin were used to visualize and quantify the amount of microparticles that marginated to the channel walls after the mixture flowed through the circular channel. After the blood preparation was made, 1 μm diameter streptavidin coated fluorescent (Excitation: 480nm, Emission: 520nm) microparticles (CP01F-12884: Bangs Laboratories, Fishers, USA) were added to produce a concentration of 27 μL of particles solution per 1mL of solution. The preparation was then put into an ultrasonic cleaner (RK-08848-10: Cole-Parmer, Montreal, Canada), which used ultrasonic sound waves to break up clumps of particles, to ensure that the fluorescent particles would not be stuck together and would be fully dispersed throughout the solution. The solution was ultrasonically cleaned for three minutes. After this, the preparation was ready for use.

These particles were chosen due to their similar size to platelets (1-2 μm), along with the fact many other studies use similar sized particles because at that size, particles at that size have been shown to marginate (Charoenphol et al. 2010). Also, because the streptavidin coating on the particles would bind tightly to the biotin embedded into the channel walls – the streptavidin-biotin bond is one of the most powerful non-covalent bonds available. Consequently, the microparticles that bind to the wall would stay there, even after the rest of the blood preparation and the free-floating particles were washed out, leaving only the ones that attached to the channel walls.

Flow control via syringe pump

To control the flow rate of the blood preparations through the channels, a syringe pump (Nexus 3000: Chemyx Inc., Stafford, USA) was used and calibrated to a 5 μL glass Hamilton syringe, by using the syringe's inner diameter to calculate how quickly the syringe pump must push on the syringe to produce a specified flow rate. The syringe and the tube connecting it to the channel were completely filled with blood, having removed any air bubbles.

Tubing

Two types of tubing were used to connect the syringe to the channel: an inch-long section of soft tubing was attached directly to the syringe and a longer length of rigid tubing (outer diameter = 1/16 in) connected the soft tubing to the channel inlet. The tube connections were tightly sealed and then glued together to ensure that there was no leakage. Once all tubing was connected, blood was then flowed through it from the syringe through the channels, with the flow rate being controlled by the syringe pump.

Cleaning

After the prepared blood sample was pumped through the channel, the channel was cleaned using another syringe filled with PBS, also controlled by the syringe pump. The PBS was forced through the channel to ensure that no blood cells were left behind and that all free-floating fluorescent microparticles were purged from the system. However, occasionally, blood would become trapped in the outlets or inlets of the channel and would require an additional flow of water to clean the channel completely.

4.1.2 Fluorescent imaging

After the blood preparation was flowed through and the channel was cleaned with PBS, the channel was examined under a LED fluorescent microscope (Axio Lab.A1: Carl Zeiss AG, Oberkochen, Germany) to image the channel and count the fluorescent particles that remained attached to the walls. To optimally view the particles, the fluorescent filter set number 09 (488009-9901-000: Carl Zeiss AG), which has an excitation band pass filter of 450-490 nm and an emission low pass filter of 515 nm and a 10x magnification lens were used. Two images (I_{z1} and I_{z2}) were taken from each channel at the same position (x,y) , but using two different focal

points (z1 and z2) within the channel, to ensure that all adhered particles were represented and in focus in at least one of the two images.

Particle counting

The computer program ImageJ was used to automatically count the number of particles in the images obtained from the fluorescent microscope. After uploading the two original images, in this case, I_{z1} and I_{z2}, as shown in Figure 22, this pair of images was overlaid on top of each other in ImageJ and resulted in the combined image I_s. If it was determined that either of the original images already contained all particles in focus, this step could be skipped, and in this case, this single original image would become I_s, for the purpose of the next step. The image I_s was then converted from a 32 bit colour image into an 8 bit black and white image (named I_{bw}). This was then sharpened using the built-in sharpen feature in ImageJ (producing image I_{bws}), which was then converted into a binary image (named I_b) using a manually set threshold that allowed only the particles to be seen. Black and white values were reversed to make the particles easier to view (resulting in image I_{final}). A particle counting algorithm in ImageJ was used to extract the size of each bright spot and the number of bright spots left in the image after conversion to binary. Several sets of images were counted by hand to ensure the accuracy of the ImageJ particle counting macro, and in all cases, the result for the hand counting and ImageJ's differed by less than 10%, and ImageJ's number was used in the final result.

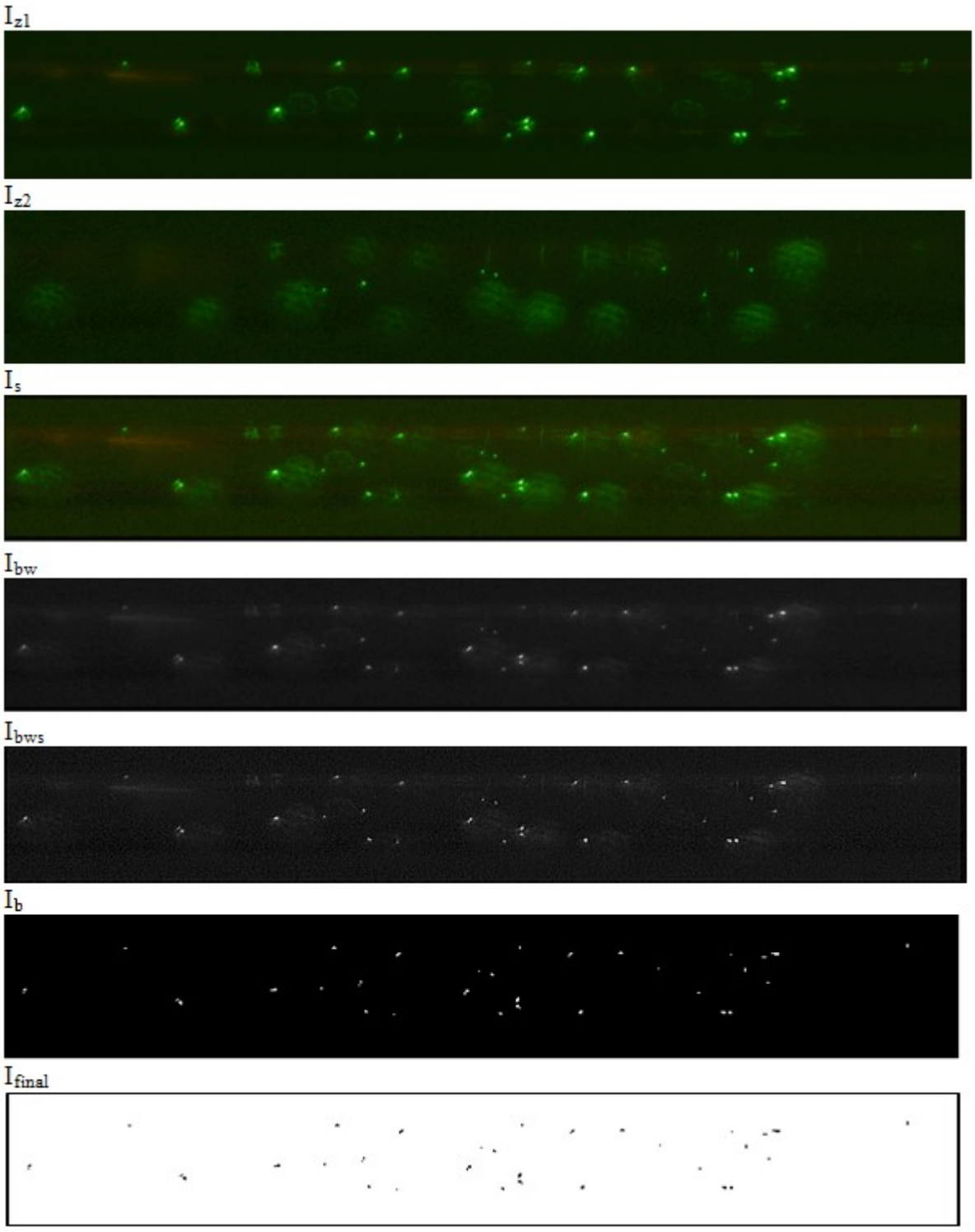

Figure 22 Image processing method used to count particle adhering to channel walls

4.1.3 Experimental method

The experiment was performed for four different target average flow velocities: 1.0, 2.0, 3.0, and 6.0 mm/s. The flow rates used to program the syringe pump were calculated using the measured diameter of the channels. Assuming incompressible and laminar flow, the flow rate Q to result in each target average velocity v was calculated using the equation:

$$Q = v\left(\frac{D^2}{2}\right)\pi \quad 8.$$

where D is the channel diameter. As each channel was fabricated individually, there was some variance in their diameter, with all variances less than 10 µm in diameter, with an average of 90 µm. Therefore, the flow rates for each channel were calculated individually. Each channel was cut into two 1cm long portions, extending from either an inlet or an outlet and a slice was cut from the central portion with a razor blade. The slice was examined under a light microscope and the area of the channel was measured. From that measurement, the flow rate was calculated. For example, a circular channel that was 90µm in diameter: to produce the target velocities of 1, 2, 3, and 6 mm/s, the flow rates of 0.36, 072, 1.44, and 2.88 µL/min, would be used, respectively. Each blood sample was flowed through their channel for one minute at the flow rate calculated for that channel for the desired velocity. This process was repeated for each concentration of Dextran. All combinations of flow velocity and dextran were repeated at least five times each and in some cases, up to eight times. Each test was performed in a new, clean channel that was fabricated no more than 48 hours beforehand.

4.2 Results of RBC aggregation on microparticle margination

The effect of Dextran on the aggregation level was found to be similar to that reported in the literature. The average level of aggregation was measured by an aggregometer (RheoScan-AnD 300 System: RheoMeditech Inc., Seoul, Korea). The output of the measurement was a quantitative number called the aggregation index. The aggregation index is a unitless number, with higher values indicating higher levels of aggregation and lower values showing lower levels of aggregation. The measurements with the aggregometer showed that at the 1.5% and 2.0% dextran w/v concentrations (Figure 23: D and E) the level of aggregation in the sampled blood preparation was near or above the average human physiological level (Figure 23: F). At 0.5% and 1.0% dextran w/v concentration (Figure 23: B and C), the level of aggregation in the sampled blood preparation was significantly lower than the average human physiological level.

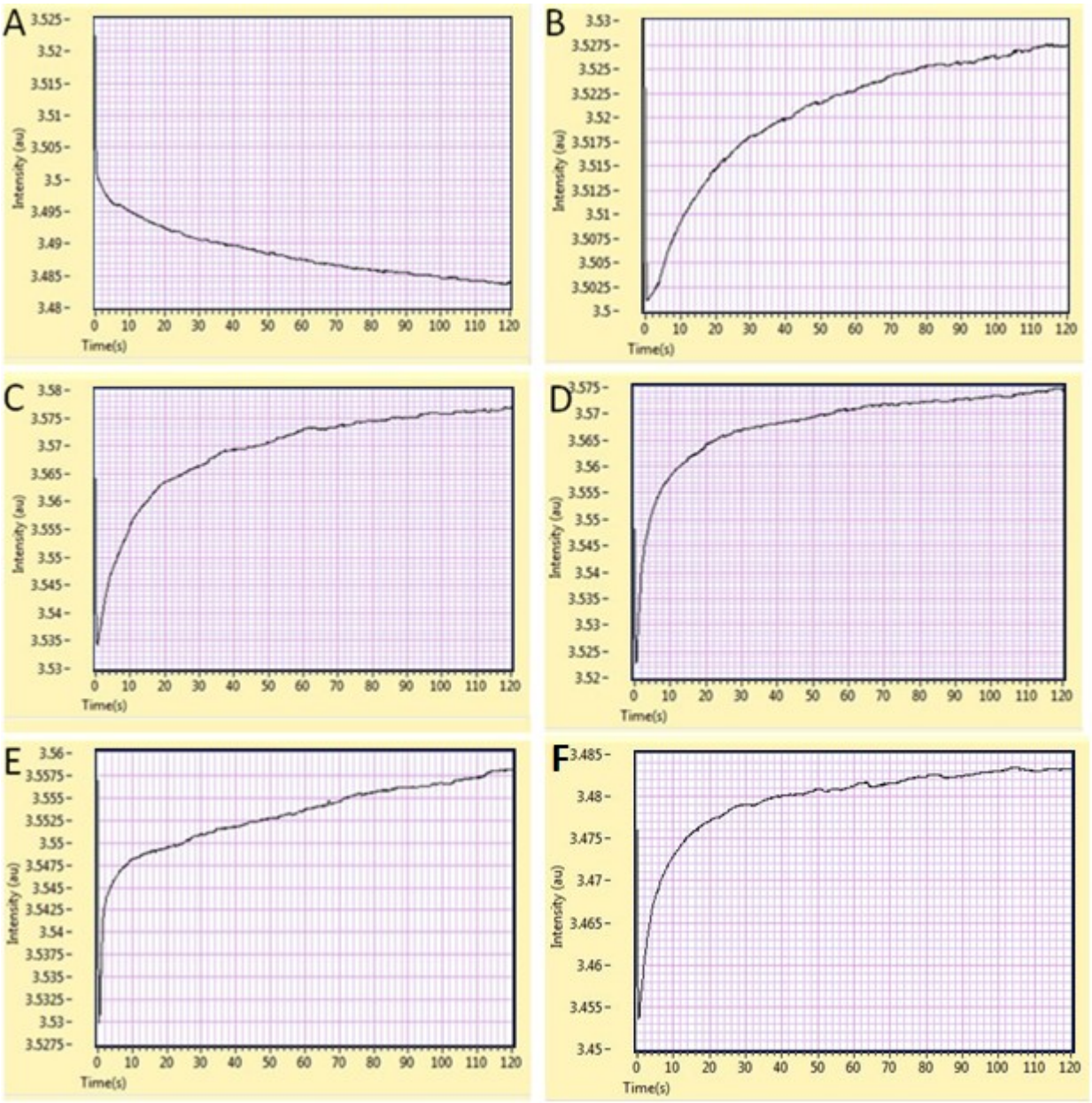

Figure 23 Sample results from the aggregometer for 0.0% (A), 0.5% (B), 1.0% (C), 1.5% (D) and 2.0% (E) dextran solutions, (F) is a result from the aggregometer for a physiological sample of whole blood. In order for the aggregometer to read the aggregation, the hematocrit of the sample must be higher than the 10% hematocrit that we used for the flow experiments, so the hematocrit of the solutions were increased to 45% hematocrit for the purposes of the test, while maintaining the relative concentrations of Optiprep and dextran.

At 0% (Figure 23: A), the aggregation index reported by the aggregometer is incorrect: the graphic analysis method used by the aggregometer to quantify aggregation does not work if

there is no presence whatsoever of a minimum spike due to the disaggregation of the red blood cells (see Figure 1). Although the reading was a false positive for high levels of aggregation, the graph of the light intensity shows that the level of aggregation of the blood sample at 0% dextran w/v concentration decreases over time, and does not increase as it did for all of the other tested samples; this indicates that there is little to no aggregation occurring in the sample. Consequently, the aggregation index of 0% dextran w/v concentration will be set to 0 and assumed to have no aggregation occurring. The average physiological level of aggregation of whole blood samples, tested before centrifugation, was measured to be 42. The averages of the aggregation indices of all tested and recorded Dextran concentrations are reported in Table 2. Because the aggregometer uses light intensity to measure the aggregation, the hematocrit of the samples must be around physiological levels to obtain an accurate reading; for samples having too low hematocrit, too much light would pass through the sample, resulting in overexposure and inaccurate readings. For this reason, samples prepared for the aggregometer measurement were made at 45% hematocrit, instead of the 10% hematocrit used in the flow experiment. The aggregometer sample had the same relative concentrations of Optiprep, and dextran with PBS as filler.

Table 2 Average aggregation indexes as measured by the aggregometer for each dextran concentration *at 0.0% dextran concentration indicates that the aggregation index was set to 0, due to the inability of the aggregometer to measure such a low aggregation rate.

Dextran Concentrations	0.0%	0.5%	1.0%	1.5%	2.0%	Physiological
Aggregation Index	0*	25.9 ± 2.4	33.1 ± 1.5	53.5 ± 2.9	48.0 ± 1.6	42 ± 1.4

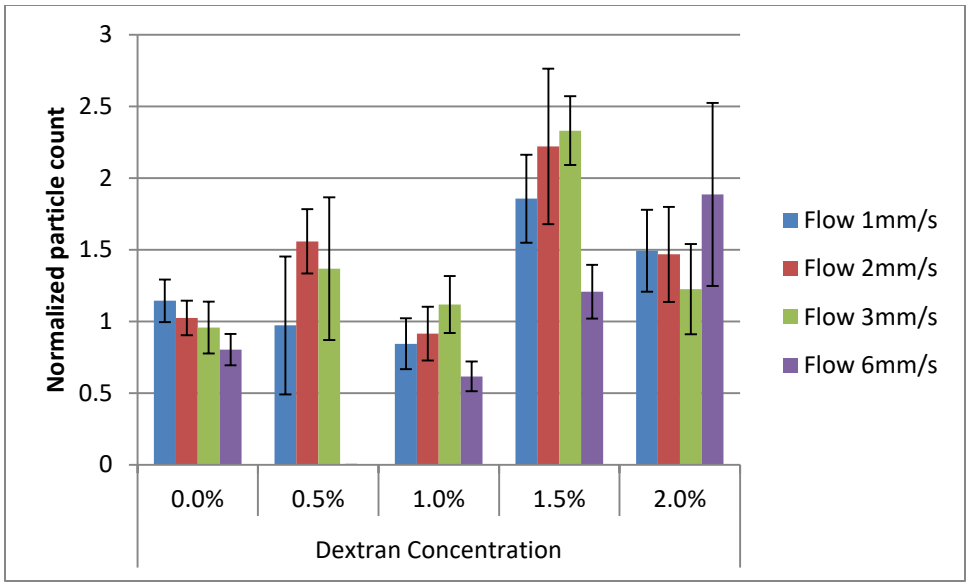

Figure 24 Average results of number of binding of microparticles for each solution of dextran and for all flow velocities. Particle counts were normalized by the average results for the 0% dextran solution.

Figure 24 presents the marginated particle counts for all blood flow experiments performed with the blood and dextran preparation. The bar graph shows the relative number of particles that were captured by the biotinylated vessel walls of each PDMS channels. The total numbers of particles captured by the channel wall in each set of experiments were normalized by the average number of particles captured by the channels flowing 0% dextran solutions in that set (e.g. for a given flow velocity). For example, if the average number of particles captured by the channels flowing 0% dextran solutions was 50, in one set, and the channel flowing the 1.5 blood -dextran preparation at 1 mm/s captured 100 particles, in the same set, the normalized particle count for the 1.5 dextran blood preparation at 1 mm/s would be 2.0.

The normalized particle counts were compared between every type of dextran solution and flow velocity used in the experiment. As can be seen from Figure 24, the particles captured for 0.5% and 1.0% were very similar with no significant difference in the number of particles binding when compared to the normalized values from the 0% dextran solution. The number of

particles captured for the 1.5% concentrations, however, were all significantly higher than the normalized values from the 0% dextran solution, except for the 1.5% dextran solution at the flow velocity of 6 mm/s, which showed no significant difference. The statistical significance was determined using two tailed t-tests, assuming un-equal variance, comparing the normalized particle count of each experimental set of dextran concentrations and flow velocities with the normalized values from the 0% dextran solution.

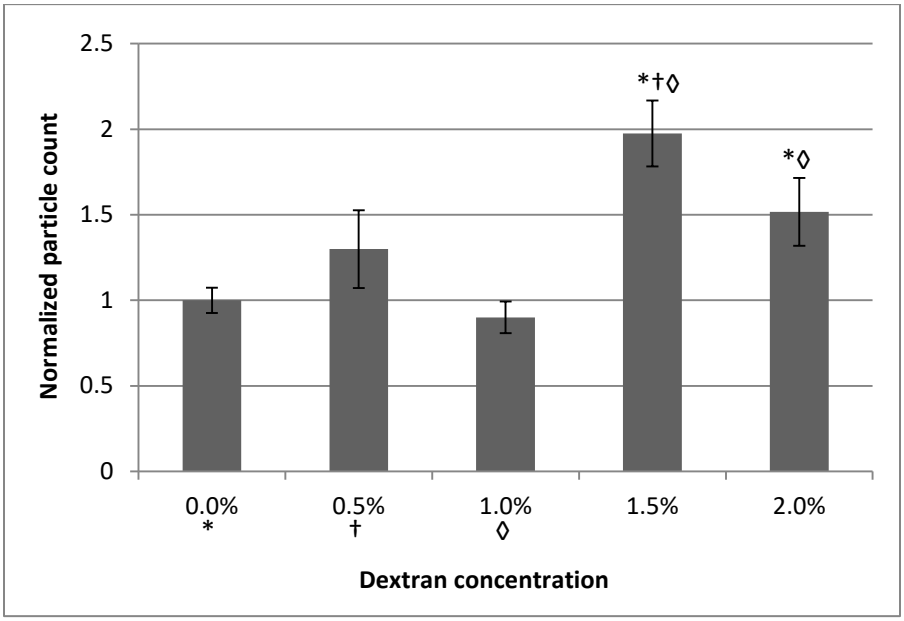

Figure 25 Average results of number of binding microparticles for each level of dextran concentration. Particle counts were normalized by the average results for the 0.0% dextran solution and the similar dextran concentrations were averaged for all flow velocities. *†◊ above a bar signifies statistically significant difference with the respective dextran concentration ($p < 0.05$)

Figure 25 is very similar to Figure 24, with the difference being that the counts for the particles that attached to the wall of the channel are averaged between all the different flow velocities for a given dextran concentration. It was found that increasing the level of aggregation in the samples above the level of 1.0% dextran significantly increased the number of microparticles that adhered to the side of the channel, indicating a higher level of margination.

The particles in all the preparations that had levels of aggregation that were below physiological levels (0%, 0.5% and 1.0%) were, on average, significantly less likely to marginate compared to particles in most of the preparations that had levels of aggregation that were above physiological levels (1.5% and 2.0%). The only non-significant difference was between the 0.5% and 2.0% dextran concentrations.

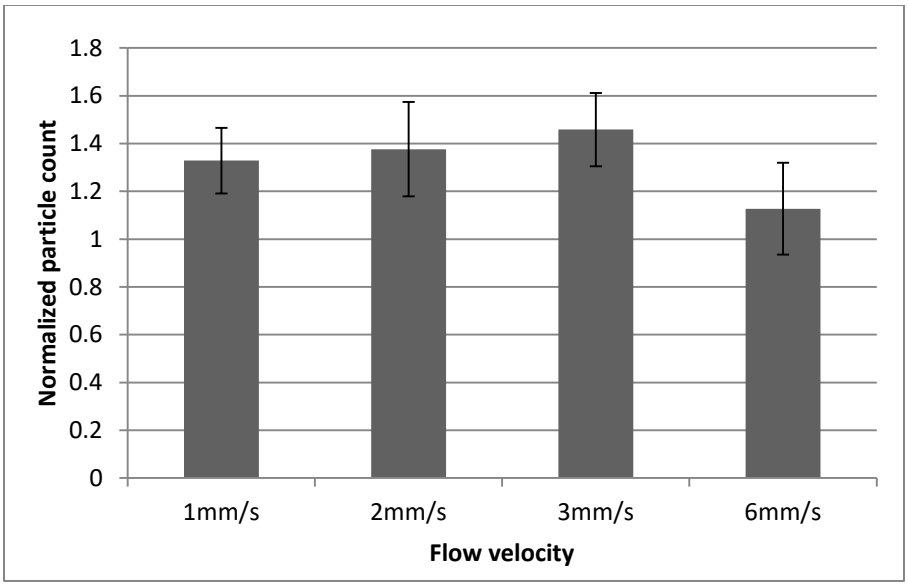

Figure 26 Average results of number of binding of microparticles for each level of flow velocity. Particle counts were normalized by the average results for the 0.0% dextran solution and the similar flow velocities for all levels of dextran concentration were averaged together

In Figure 26, the normalized particle counts were averaged between all different dextran concentrations for each flow velocity. Based on the data acquired, the flow velocity of the blood-dextran preparation through the channels was found to have no significant effect on the level of margination of the microparticles in the preparation.

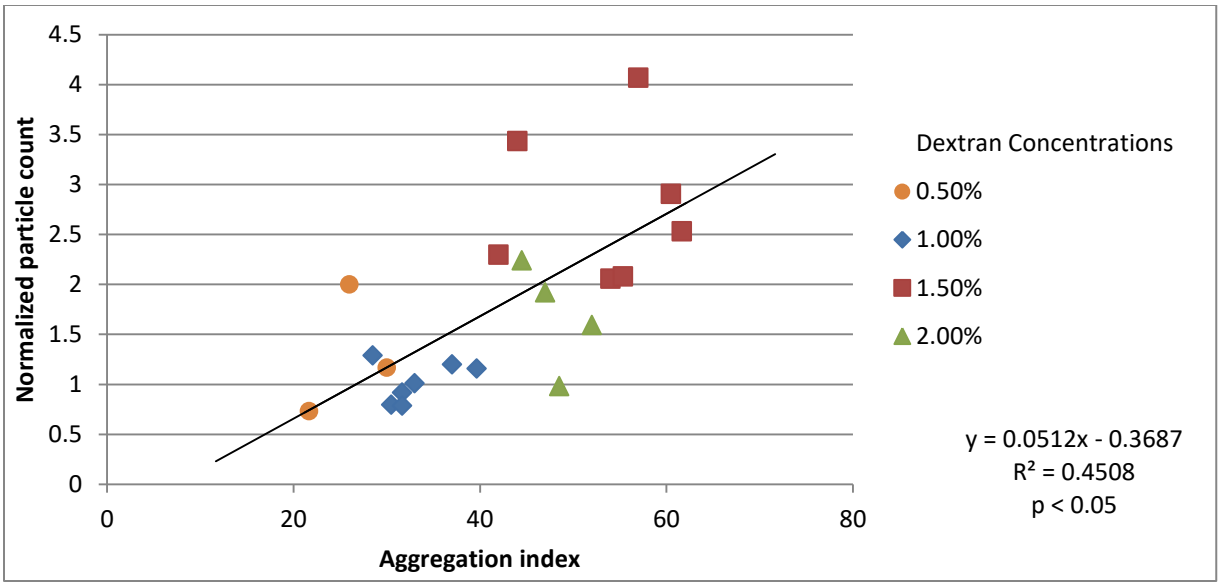

Figure 27 Scatterplot of aggregation index against the normalized particle count of the particles adhering the channel walls, with line of best fit.

Figure 27 shows the comparison of the aggregation index of each sample and the normalized particle count for that particular sample's flow test. The normalized particle counts positively correlate with the aggregation indices and fall along a line of best fit with a slope of 0.05 and an R^2 fit value of 0.45. The dextran concentration for each sample is also indicated, and each group of dextran concentration clusters together on the scatterplot, owing to the fact that the dextran concentration directly affects the level of aggregation in each sample similarly.

4.3 Discussion

The macromolecule dextran 500 was used in this study to modify the level of aggregation of the tested blood suspensions. The level of aggregation in the samples was found to increase with increasing dextran concentration up to 1.5% w/v, after which it decreased. This trend supports previous experiments which found that beyond a certain concentration, dextran begins to have an inhibitory effect on red blood cell aggregation (Baskurt et al. 2012). The depletion layer theory of aggregation offers an explanation for this trend as follows. Normally, aggregation is caused by an attractive force between two red blood cells that is a result of an osmotic pressure difference that forms between the intercellular polymer-poor depletion zone between the surfaces of the two cells and the polymer-rich zone of the surrounding media (Neu et al. 2008). At lower concentrations, Dextran will increase the aggregation force between the two cells by increasing the concentration in the polymer-rich zone of the surrounding media, thereby increasing the osmotic pressure difference. However when the dextran concentration is too high, it will penetrate the normally polymer-poor intercellular depletion zone, increasing the concentration there and reducing the osmotic pressure difference (Neu et al. 2008).

This increase-decrease pattern matches our measurements closely; however, previous studies have come to little consensus as to the point at which the dextran concentration turns to inhibition. Figure 28 shows the measurements from two different studies of the aggregation index curve caused by dextran 500. In Figure 28 (A) (Neu et al. 2008) the peak of aggregation occurs at around 1.0% dextran concentration. In Figure 27 (B) (Pearson & Lipowsky 2000) the curve shape is very different, with the aggregation index dropping off more significantly at high concentrations. The peak of aggregation occurs at approximately 3.0% dextran concentration, a much higher value than was found by Neu et al. (2008).

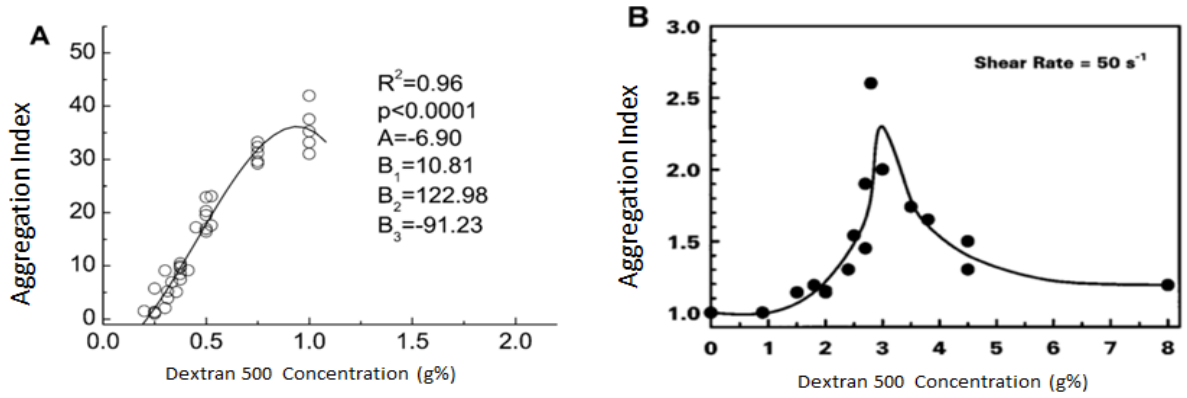

Figure 28 Comparison of aggregation peaks caused by Dextran 500 in (A) (Neu et al. 2008) **and (B)** (Pearson & Lipowsky 2000)**.**

The results measured from the aggregometer used in the present experiments falls in between those of the previously mentioned studies, with the aggregation peaking at 52.0 and occurring at 1.73% dextran, as shown in Figure 29. The differences among these studies could be explained by the use of different techniques to measure the aggregation index. For example, Neu et al., (2008) used a cone-plate intrument to evenly shear the blood sample at 600 s^{-1} briefly, after which the light transmission was measured and integrated for 10 seconds giving a value for the aggregation index. Pearson & Lipowsky, (2000) also used a cone-plate instrument, however they applied a shear rate of only 50 s^{-1}, much lower than that used by Neu et al. The technique used in our experiments involved using a magnetic stir stick spinning at 800 rpm and using a blood sample of just 6µl. Additionally, the time over which the light intensity difference was measured was much greater in the present study (120 second instead of 10 seconds).

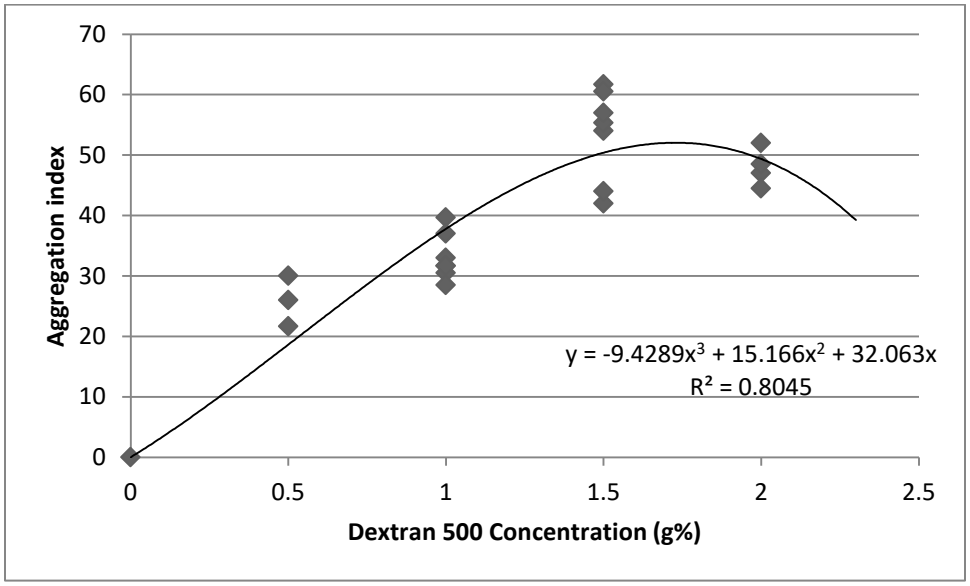

Figure 29 Scatterplot of aggregation index caused by Dextran 500 in our experiments, with a peak in aggregation falling between 1.5% and 2.0% dextran. A third order polynomial line of best fit is fitted to the data.

The third objective of this study was to measure particle margination for varying levels of aggregation (due to different concentrations of dextran) and for different flow velocities. As was shown previously in Figure 26, no correlation was found between particle margination and flow velocity when averaging the results across all dextran concentrations. Some correlation was apparent, however, when considering the results for the 0% dextran solutions alone, as shown in Figure 30. For this zero aggregation case, margination was found to decrease with increasing flow rate, although the trend was not found to be statistically significant. At 0% dextran concentration there was no aggregation occurring between the RBCs, and consequently the observed margination for this case could not be dependent on aggregation, thus isolating the effect of flow rate. It is logical that higher flow rates would result in lower particle attachment, as they likely reduce the amount of particles adhering to the side of the channel by increasing the shear rate at the channel walls, potentially knocking off particles or making it more difficult for

them to adhere. This result, however, is a weak correlation, and it is recommended that more testing be done to understand if in fact there is any significant correlation and explore the mechanisms behind the potential correlation.

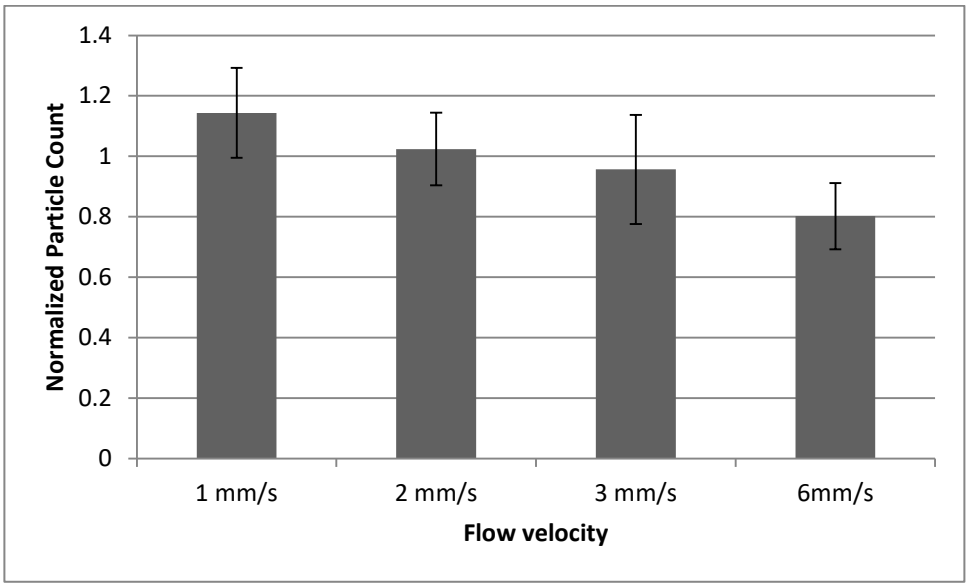

Figure 30 Averaged normalized particle count against flow velocity for all 0% Dextran 500 concentrations

For the 1.0% and 1.5% dextran concentrations, the opposite trend was observed: for the flow velocities 1, 2, and 3mm/s, the normalized particle counts increased with increasing flow rate (Figure 31). This was possibly due to the fact that with an increase in flow rate, more particles will be present in the channel over a period of time, meaning more particles are available to adhere to the channel walls. When the flow velocity increased to 6mm/s, however, the normalized particle count dropped and was, in fact; significantly lower from the measurements made at 3 mm/s. This may be because when the flow velocity reached 6mm/s, the shear rate became too high for the particles to easily bind to the wall, even with the increased amount of particles available, reducing the normalized particle count. This trend, however, was

only observed for the 1.0% and 1.5% dextran concentrations, and not for the lower concentrations.

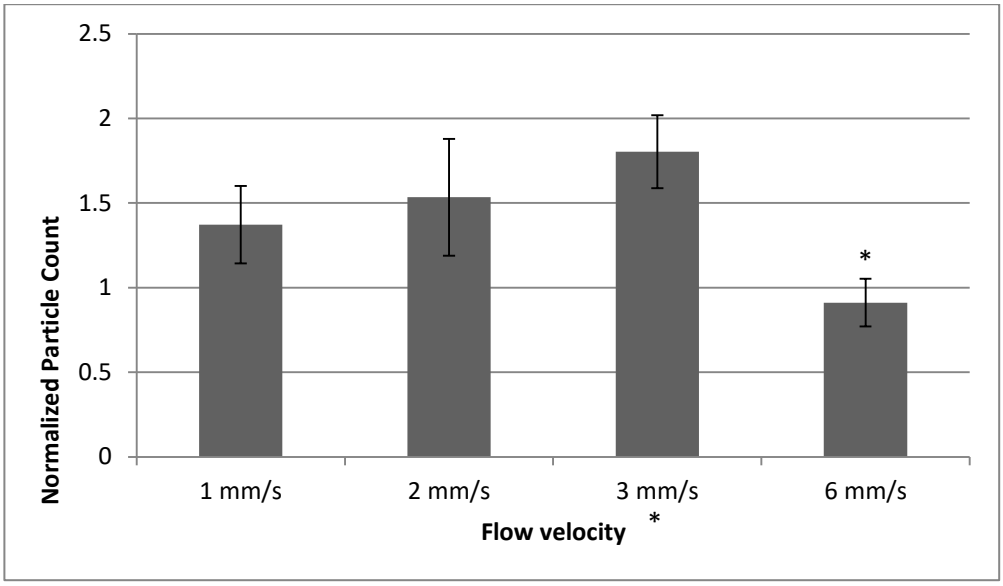

Figure 31 Normalized particle counts against flow velocity averaged for all 1.0% and 1.5% dextran 500 concentrations. * signifies statistically significant difference ($p < 0.05$)

As was observed from Figure 25, the margination levels for the 1.5% and 2.0% dextran concentrations were statistically higher than those for the 0%, 0.5% and 1.0% dextran concentrations. This supports the hypothesis that aggregation can influence the level of margination. Notably, there was a significant jump in the normalized particle counts from the 1.0% dextran to the 1.5% dextran concentrations. The aggregation index of these two levels of dextran coincides with the average aggregation index of whole, physiological blood. This indicates that aggregation plays an important role in physiological margination. It has already been shown that aggregation plays an important role in the human body's immune system (Baskurt et al. 2009), and the present results indicate that one mechanism by which it does this is by increasing margination, which can help platelets and immune cells travel to the site of

inflammation to support the healing and immune defence process. This potentially explains why an increase in aggregation is so often observed in different pathological conditions.

Figure 27 showed that the level of aggregation is roughly linearly correlated with the normalized particle count and thus the level of margination in the channel. This result agrees with the results of other studies that examined the effect of aggregation on margination within different channel geometries (e.g. a Couette cylinder (Guilbert 2009) or parallel plate flow chamber (Namdee et al. 2013)). These studies similarly found that increased aggregation is correlated with increased margination, adding to our confidence that our results are correct and reproducible in other systems and geometries.

While this study provided the first experimental evidence that aggregation increases margination in round channels, the measurement of margination could be improved upon in future studies. Instead of measuring the after-effects of flowing the fluorescent microparticles through the channels, one could visualize them in real time, using micro particle image velocimetry (μPIV) and high-speed image microscopy. By these means, one could quantify the velocity vectors of the particles imaged within the vessel. This would allow us to examine the lateral velocities of the particles in the fluid and see more precisely how they are affected by changes in the level of aggregation.

5 Conclusion

In the first part of this work, we presented an optimized procedure for making wafers using photolithography and a new combination of techniques to fabricate biotinylated PDMS round channels from fabricated rectangular channels. This combination technique could be used for other future studies to examine particle adherence to the walls in a circular channel.

In conclusion, we have (1) determined an appropriate methodology to fabricate circular microchannels in PDMS by identifying the optimal method to produce a rectangular channel, and then coating the channel with PDMS using the air pressure method in order to circularize them. (2) In order to measure levels of margination, we developed a methodology to capture particles that have migrated toward the wall, using streptavidin-coated particles that bond to biotin embedded in the walls of the circular channels. Finally, (3) we performed a comparison of particle migration in round microchannels for different levels of RBC aggregation and for different flow velocities and quantified the results using image processing techniques.

It was found that the flow velocities for the average of all dextran concentrations did not have any significant effect on the level of margination. Considering flow velocity of only the 0% dextran concentration, however, a slight decrease in margination was found for increasing flow velocity, whereas flow velocity for the 1.0% and 1.5% dextran concentrations, the concentrations nearest physiological aggregation levels, the opposite was found, with margination increasing with flow rate until a sudden drop-off occurred at the flow rate corresponding to 6mm/s average velocity.

We have also shown that the level of margination is positively correlated with the level of aggregation and that margination was found to be especially sensitive to aggregation level in the range of physiological aggregation levels of whole blood. This suggests that aggregation plays an

important role in margination *in vivo*, and that this influence may be one mechanism by which aggregation supports immune response: by increasing margination, the movement of white blood cells and platelets to sites of injury is increased. The fact that flow velocity also had its largest effect on margination near these physiological levels at 1.0 and 1.5% dextran, adds more significance to this finding.

It is our hope that these findings could be used to further the understanding the roles of aggregation and margination in the body and their importance toward inflammation and immune response.

6 References

Abdelgawad, Mohamed, Wei-Yin Chien, Ting-Kai Liang, and Yu Sun. 2010. "Microfluidic Platform with Circular Microchannels for Facile Cell Trapping and Single Cell Analysis." *14th International Conference on Miniaturized Systems for Chemistry and Life Science* (October): 235–37. http://www.rsc.org/binaries/LOC/2010/PDFs/Papers/081_0922.pdf.

Abdelgawad, Mohamed, Chun Wu, Wei Yin Chien, and Yu Sun. 2010. "A Fast and Simple Method to Fabricate Circular Microchannels in Polydimethylsiloxane (PDMS)." *Proceedings of the IEEE International Conference on Micro Electro Mechanical Systems (MEMS)*: 1071–74.

Apolito, Rosa D et al. 2015. "Red Blood Cells Affect the Margination of Microparticles in Synthetic Microcapillaries and Intravital Microcirculation as a Function of Their Size and Shape." *Journal of Controlled Release* 217: 263–72. http://dx.doi.org/10.1016/j.jconrel.2015.09.013.

Baskurt, Oguz K. et al. 2009. "New Guidelines for Hemorheological Laboratory Techniques." *Clinical Hemorheology and Microcirculation* 42(2): 75–97.

Baskurt, Oguz K., Björn Neu, and Herbert J. Meiselman. 2012. *Red Blood Cell Aggregation*. CRC Press.

Betancourt, Tania, and Lisa Brannon-peppas. 2006. "Micro- and Nanofabrication Methods in Nanotechnological Medical and Pharmaceutical Devices." *International Journal of Nanomedicine* (February 2006).

Blombäck, Birger. 1996. "Fibrinogen and Fibrin - Proteins with Complex Roles in Hemostasis and Thrombosis." *Thrombosis Research* 83(1): 1–75.

Carboni, Erik et al. 2014. "Particle Margination and Its Implications on Intravenous Anticancer

Drug Delivery." *AAPS PharmSciTech* 15(8): 762–71. http://www.ncbi.nlm.nih.gov/pubmed/24687242.

Charoenphol, Phapanin, Ryan B. Huang, and Omolola Eniola-Adefeso. 2010. "Potential Role of Size and Hemodynamics in the Efficacy of Vascular-Targeted Spherical Drug Carriers." *Biomaterials* 31(6): 1392–1402. http://dx.doi.org/10.1016/j.biomaterials.2009.11.007.

Decuzzi, Paolo, S. Lee, B. Bhushan, and M. Ferrari. 2005. "A Theoretical Model for the Margination of Particles within Blood Vessels." *Annals of Biomedical Engineering* 33(2): 179–90.

Doshi, Nishit et al. 2010. "Flow and Adhesion of Drug Carriers in Blood Vessels Depend on Their Shape: A Study Using Model Synthetic Microvascular Networks." *Journal of Controlled Release* 146(2): 196–200. http://dx.doi.org/10.1016/j.jconrel.2010.04.007.

Fenn, Wallace O. 1921. "Hemolysis of Erythrocytes in Contact with Glass." *Biochem*: 271–86.

Freund, Jonathan B. 2007. "Leukocyte Margination in a Model Microvessel." *Physics of Fluids* 19(2): 0–13.

Gentile, F. et al. 2008. "The Effect of Shape on the Margination Dynamics of Non-Neutrally Buoyant Particles in Two-Dimensional Shear Flows." *Journal of Biomechanics* 41(10): 2312–18.

Guilbert, Cyrille. 2009. Masters thesis "Influence de L'agrégation Érythrocytaire Sur La Migration Axiale de Microparticules Simulant Des Plaquettes Sanguines."

Hall, John E, and Arthur C Guyton. 2011. *Textbook of Medical Physiology*. 12th ed. Philadelphia: Saunders Elsevier.

Huang, Bo et al. 2006a. "Phospholipid Biotinylation of Polydimethylsiloxane (PDMS) for Protein Immobilization." *Lab on a chip*.

———. 2006b. “Phospholipid Biotinylation of Polydimethylsiloxane (PDMS) for Protein Immobilization.” *Lab on a chip* 6(3): 369–73.

Krogh, Magnus. 2003. “My Little Guide to Soft Lithography.”

Kumar, Amit, and Michael D. Graham. 2011. “Segregation by Membrane Rigidity in Flowing Binary Suspensions of Elastic Capsules.” *Physical Review E - Statistical, Nonlinear, and Soft Matter Physics* 84(6): 1–17.

Lee, Jihoon et al. 2013. “Effect of Thermal Treatment on the Chemical Resistance of Polydimethylsiloxane for Microfluidic Devices.” *Journal of Micromechanics and Microengineering* 23(3): 35007. http://stacks.iop.org/0960-1317/23/i=3/a=035007?key=crossref.ce5bccaf614f12853596f8e4558bd534.

Lee, Tae-Rin et al. 2013. “On the near-Wall Accumulation of Injectable Particles in the Microcirculation: Smaller Is Not Better.” *Scientific Reports* 3: 2079. http://www.pubmedcentral.nih.gov/articlerender.fcgi?artid=3693098&tool=pmcentrez&rendertype=abstract.

Martinez-duarte, Rodrigo. 2014. “SU-8 Photolithography as a Toolbox for Carbon MEMS.” *Micromachines*: 766–82.

MicroChem. 2012. “Lithography Trouble Shooter.”

———. *SU-8 Negative Tone Photoresist Formulations 50-100*.

Namdee, Katawut, Alex J. Thompson, Phapanin Charoenphol, and Omolola Eniola-Adefeso. 2013. “Margination Propensity of Vascular-Targeted Spheres from Blood Flow in a Microfluidic Model of Human Microvessels.” *Langmuir* 29(8): 2530–35.

Nash, Gerard B., Tim Watts, Colin Thornton, and Mostafa Barigou. 2008. “Red Cell Aggregation as a Factor Influencing Margination and Adhesion of Leukocytes and

Platelets." *Clinical Hemorheology and Microcirculation* 39(1–4): 303–10.

Neu, Bjorn, Rosalinda Wenby, and Herbert J Meiselman. 2008. "Effects of Dextran Molecular Weight on Red Blood Cell Aggregation." *Biophysical journal* 95(September): 3059–65.

Pan, Wenxiao, Dmitry A. Fedosov, Bruce Caswell, and George Em Karniadakis. 2011. "Predicting Dynamics and Rheology of Blood Flow: A Comparative Study of Multiscale and Low-Dimensional Models of Red Blood Cells." *Microvascular Research* 82(2): 163–70. http://dx.doi.org/10.1016/j.mvr.2011.05.006.

Pandey, Rahul, and Jacinta C Conrad. 2012. "Effects of Attraction Strength on Microchannel Flow of Colloid – Polymer Depletion Mixtures." *Soft Matter* 8: 10695–703.

Pearson, Mark J, and Herbert H Lipowsky. 2000. "Influence of Erythrocyte Aggregation on Leukocyte Margination in Postcapillary Venules of Rat Mesentery." *Am J Physiol Heart Circ Physiol* 279: 1460–71.

Perry, Hannah et al. 2007. "Simple Fabrication Technique for Rapid Prototyping of Seamless Cylindrical Microchannels in Polymer Substrates." *Review of Scientific Instruments* 78(4): 6–9.

Pinto, Vânia C, Paulo J Sousa, Vanessa F Cardoso, and Graça Minas. 2014. "Optimized SU-8 Processing for Low-Cost Microstructures." *Micromachines*: 738–55.

Rogers, John A., and Ralph G. Nuzzo. 2005. "Recent Progress in Soft Lithography." *Materials Today* 8(2): 50–56. http://dx.doi.org/10.1016/S1369-7021(05)00702-9.

San-miguel, Adriana, and Hang Lu. 2013. "Microfluidics as a Tool for C . Elegans Reseach." *Wormbook*: 1–19.

Shin, Sehyun, Yijie Yang, and Jang-soo Suh. 2009. "Measurement of Erythrocyte Aggregation in a Microchip Stirring System by Light Transmission." *Clinical Hemorheology and*

Microcirculation 41: 197–207.

Simmonds, Michael J, Rhys Christy, Sonya M Marshall-gradisnik Herbert J Meiselman, and Oguz K Baskurt. 2011. "Red Blood Cell Aggregation Parameters Measured by Capillary Tube Aggregometer Using Venous and Capillary Blood Samples." *Korea-Australia Rheology Journal* 23(4): 205–10.

Toy, Randall et al. 2011. "The Effects of Particle Size, Density and Shape on Margination of Nanoparticles in Microcirculation." *Nanotechnology* 22(11): 115101.

Yang, Xiaoxi, Omid Forouzan, Jennie M Burns, and Sergey S Shevkoplyas. 2011. "Traffic of Leukocytes in Microfluidic Channels with Rectangular and Rounded Cross-Sections." *Lab on a chip* 11(19): 3231–40.